



TITLE:

# Tomato root-associated Sphingobium harbors genes for catabolizing toxic steroidal glycoalkaloids

AUTHOR(S):

Nakayasu, Masaru; Takamatsu, Kyoko; Kanai, Keiko;  
Masuda, Sachiko; Yamazaki, Shinichi; Aoki, Yuichi; Shibata,  
Arisa; ... Shirasu, Ken; Yazaki, Kazufumi; Sugiyama, Akifumi

---

CITATION:

Nakayasu, Masaru ...[et al]. Tomato root-associated Sphingobium harbors genes for catabolizing toxic steroidal glycoalkaloids. *mBio* 2023, 14(5): e00599-23.

ISSUE DATE:

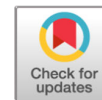
2023-10-31

URL:

<http://hdl.handle.net/2433/285970>

RIGHT:

© 2023 Nakayasu et al.; This is an open-access article distributed under the terms of the Creative Commons Attribution 4.0 International license.



8 | Physiology and Metabolism | Research Article

# Tomato root-associated *Sphingobium* harbors genes for catabolizing toxic steroidal glycoalkaloids

Masaru Nakayasu,<sup>1</sup> Kyoko Takamatsu,<sup>1</sup> Keiko Kanai,<sup>1</sup> Sachiko Masuda,<sup>2</sup> Shinichi Yamazaki,<sup>3</sup> Yuichi Aoki,<sup>3,4</sup> Arisa Shibata,<sup>2</sup> Wataru Suda,<sup>5</sup> Ken Shirasu,<sup>2</sup> Kazufumi Yazaki,<sup>1</sup> Akifumi Sugiyama<sup>1</sup>

**AUTHOR AFFILIATIONS** See affiliation list on p. 17.

**ABSTRACT** Plant roots exude various organic compounds, including plant specialized metabolites (PSMs), into the rhizosphere. The secreted PSMs enrich specific microbial taxa to shape the rhizosphere microbiome, which is crucial for the healthy growth of the host plants. PSMs often exhibit biological activities; in turn, some microorganisms possess the capability to either resist or detoxify them. Saponins are structurally diverse triterpene-type PSMs that are mainly produced by angiosperms. They are generally considered as plant defense compounds. We have revealed that  $\alpha$ -tomatine, a steroid-type saponin secreted from tomato (*Solanum lycopersicum*) roots, increases the abundance of *Sphingobium* bacteria. To elucidate the mechanisms underlying the  $\alpha$ -tomatine-mediated enrichment of *Sphingobium*, we isolated *Sphingobium* spp. from tomato roots and characterized their saponin-catabolizing abilities. We obtained the whole-genome sequence of *Sphingobium* sp. RC1, which degrades steroid-type saponins but not oleanane-type ones, and performed a gene cluster analysis together with a transcriptome analysis of  $\alpha$ -tomatine degradation. The *in vitro* characterization of candidate genes identified six enzymes that hydrolyzed the different sugar moieties of steroid-type saponins at different positions. In addition, the enzymes involved in the early steps of the degradation of sapogenins (i.e., aglycones of saponins) were identified, suggesting that orthologs of the known bacterial steroid catabolic enzymes can metabolize sapogenins. Furthermore, a comparative genomic analysis revealed that the saponin-degrading enzymes were present exclusively in certain strains of *Sphingobium* spp., most of which were isolated from tomato roots or  $\alpha$ -tomatine-treated soil. Taken together, these results suggest a catabolic pathway for highly bioactive steroid-type saponins in the rhizosphere.

**IMPORTANCE** Saponins are a group of plant specialized metabolites with various bioactive properties, both for human health and soil microorganisms. Our previous works demonstrated that *Sphingobium* is enriched in both soils treated with a steroid-type saponin, such as tomatine, and in the tomato rhizosphere. Despite the importance of saponins in plant–microbe interactions in the rhizosphere, the genes involved in the catabolism of saponins and their aglycones (sapogenins) remain largely unknown. Here we identified several enzymes that catalyzed the degradation of steroid-type saponins in a *Sphingobium* isolate from tomato roots, RC1. A comparative genomic analysis of *Sphingobium* revealed the limited distribution of genes for saponin degradation in our saponin-degrading isolates and several other isolates, suggesting the possible involvement of the saponin degradation pathway in the root colonization of *Sphingobium* spp. The genes that participate in the catabolism of sapogenins could be applied to the development of new industrially valuable sapogenin molecules.

**KEYWORDS** degradation enzymes, rhizosphere, steroid-type saponins, *Sphingobium*, tomato

**Invited Editor** Paula Welander, Stanford University, Stanford, California, USA

**Editor** Dianne K. Newman, California Institute of Technology, Pasadena, California, USA

Address correspondence to Masaru Nakayasu, [masaru\\_nakayasu@rish.kyoto-u.ac.jp](mailto:masaru_nakayasu@rish.kyoto-u.ac.jp), or Akifumi Sugiyama, [akifumi\\_sugiyama@rish.kyoto-u.ac.jp](mailto:akifumi_sugiyama@rish.kyoto-u.ac.jp).

The authors declare no conflict of interest.

See the funding table on p. 18.

**Received** 8 March 2023

**Accepted** 8 August 2023

**Published** 29 September 2023

Copyright © 2023 Nakayasu et al. This is an open-access article distributed under the terms of the [Creative Commons Attribution 4.0 International license](https://creativecommons.org/licenses/by/4.0/).

Plant roots secrete an array of organic compounds, including biologically active plant specialized metabolites (PSMs), into the rhizosphere, which is the zone of soil surrounding the roots (1). The secreted PSMs have a wide range of ecological functions that allow them to mediate the interaction between the host plants and their surrounding organisms (2, 3). In the last decade, PSMs have been reported to shape microbial communities called the microbiome, and to enrich specific taxa in the rhizosphere and roots (4–6). Moreover, the root-associated microbiome formed by PSMs can improve the growth of the host plants under environmental stresses, such as nutrient deficiency, dryness, and attack by pathogens and herbivores (7–11).

Saponins are PSMs with diverse chemical structures (Fig. 1) that act as natural surfactants and are broadly distributed in angiosperm plants (12). The biosynthesis of saponins is derived from the mevalonate pathway and is initiated by the formation of a triterpenoid backbone, followed by further chemical decorations, such as oxidation and glycosylation (13, 14). Structural diversity is provided by the variable cyclization pattern of 2,3-oxidosqualene, as the last common precursor of all triterpenes except hopanoids, which are directly formed from squalene; furthermore, the diverse cyclizations of saponins are catalyzed by the oxidosqualene cyclase (OSC) group of enzymes. For example, the cucurbitadienol (cucurbitane-type), dammarenediol-II (dammarane-type), and  $\beta$ -amyrin (oleanane-type) compounds are formed by specific OSCs and are finally converted to ginsenosides, mogrosides, and soyasaponins, which are triterpenoid

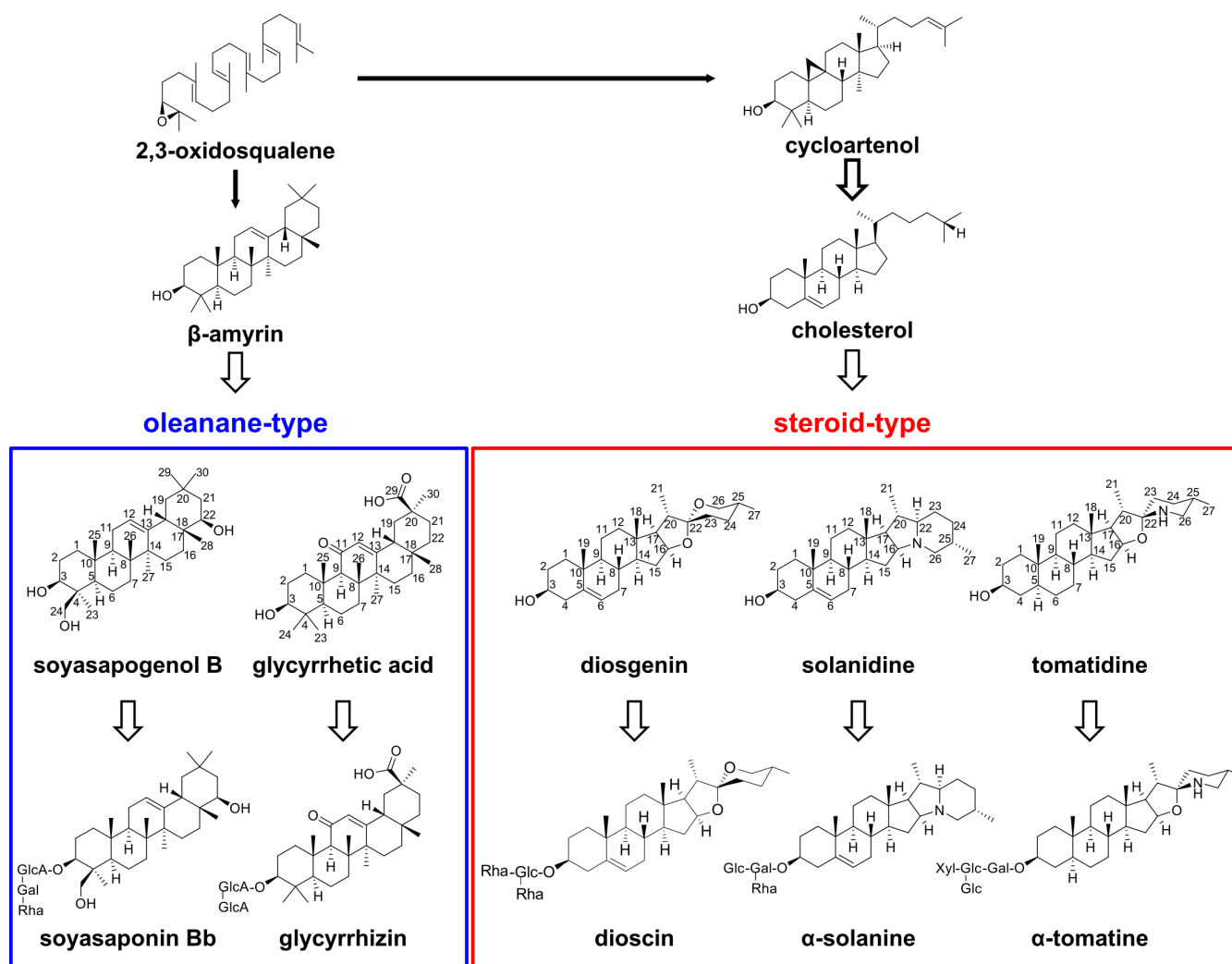


FIG 1 Biosynthesis of steroid- and oleanane-type saponins in plants. The solid and white arrows indicate one and multiple reaction steps, respectively.

saponins of Chinese ginseng (*Panax notoginseng*), monk fruit (*Siraitia grosvenorii*), and several *Fabaceae* plants (including soybean [*Glycine max*]), respectively (15). Glycyrrhizin is another oleanane-type triterpenoid saponin that is used as a natural sweetener and is found only in licorice (*Glycyrrhiza* spp., *Fabaceae*) (16). In addition, the cyclization to cycloartenol eventually leads to the production of steroid-type saponins via cholesterol synthesis; these saponins are classified into two groups: steroidal saponins and steroidal glycoalkaloids (SGAs), with the former including dioscin in *Dioscorea* plants (17) and the latter encompassing a nitrogen atom in molecules that mainly occur as  $\alpha$ -tomatine in *Solanum lycopersicum* (tomato) and as  $\alpha$ -solanine and  $\alpha$ -chaconine in *S. tuberosum* (potato) (18, 19).

According to the molecular species, saponins exhibit foaming and emulsifying properties; hemolytic and cytotoxic activities; pharmacological actions; taste properties; and toxicity against microbes, insects, and mollusks (20). Moreover, because of their allelopathic activities and inhibitory effects against plant pathogens and herbivores, saponins are thought to serve as chemical-defense compounds that protect the host plants (21–23). For instance, a tomato mutant with a low  $\alpha$ -tomatine content exhibited increased susceptibility to the larvae of the generalist herbivore *Spodoptera litura* (24). In oat (*Avena strigosa*), a mutant lacking avenacin, which is an oleanane-type triterpenoid, showed impaired resistance to various fungal pathogens (25). Our previous works have shown that soybean (*Glycine max*) and tomato secrete soyasaponins and  $\alpha$ -tomatine from their roots into the rhizosphere, and that soyasaponins and  $\alpha$ -tomatine specifically enriched the rhizosphere in *Novosphingobium* and *Sphingobium*, respectively, both of which are genera belonging to family *Sphingomonadaceae* (26–28). These studies revealed new functions of saponin in microbiome formation, in addition to their roles in host plant defense, as well as a relationship between their chemical structures and their biological effects (29).

Saponins secreted into the rhizosphere are degraded by soil microorganisms. *Arthrobacter* and *Serratia* isolated from the soils surrounding green potato peel degraded  $\alpha$ -solanine and  $\alpha$ -chaconine (30), whereas *Sphingobium* spp. isolated from tomatine-treated soil degraded  $\alpha$ -tomatine (28). The aglycones of saponins, such as solanidine and tomatidine (which are collectively called sapogenins), do not accumulate in these bacteria, suggesting that soil bacteria have the ability to metabolize sapogenins. In contrast, intestinal microorganisms can hydrolyze the glycoside bonds of saponins to produce sapogenins, which are not further degraded; rather, they are adsorbed from the intestine (31–33). These findings suggest that soil bacteria, in contrast with intestinal bacteria, possess unique catabolic enzymes for the degradation of saponins. Many microbial glycoside hydrolases (GHs), which catalyze saponin deglycosylation steps, have been identified, especially from fungal pathogens (34–38). In contrast, the microbial metabolic pathway for sapogenin degradation has not been uncovered. The steroid (but not sapogenin)-degradation enzymes that are present in *Comamonas testosteroni* TA441 have been well studied; moreover, their orthologs in the *Novosphingobium tardaugens* strain ARI-1 (NBRC 16725) have also been identified via *in silico* analysis (39, 40). In the present study, we sequenced the genome of *Sphingobium* spp. isolated from tomato roots as well as  $\alpha$ -tomatine-treated soils, and identified the enzymes responsible for the degradation of both the sugar moieties and the tomatidine backbone of  $\alpha$ -tomatine. A comparative genomic analysis revealed the limited distribution of  $\alpha$ -tomatine-metabolizing genes in *Sphingobium*, suggesting the molecular mechanism via which root-associated microbes manage the bioactive PSMs secreted from host plants.

## RESULTS

### Isolation of *Sphingobium* spp. and their saponin degradation activities

We reported previously that three *Sphingobium* strains isolated from  $\alpha$ -tomatine-treated soils degraded  $\alpha$ -tomatine (28). Here, we isolated additional 11 *Sphingobium* strains from  $\alpha$ -tomatine-treated soils and one strain from tomato roots (Table S1). We then measured the  $\alpha$ -tomatine-degradation activities using those *Sphingobium* strains. The incubation

of these resting cells with  $\alpha$ -tomatine (as a substrate) revealed that all strains degraded this compound (Fig. S1). Using one strain from tomato roots termed RC1, we evaluated the substrate specificity of its degradation activities toward several saponins and their aglycones (Fig. 1). RC1 degraded steroid-type saponins, i.e.,  $\alpha$ -tomatine,  $\alpha$ -solanine, and dioscin; as well as their respective sapogenins: tomatidine, solanidine, and diosgenin (Fig. 2). In turn, RC1 did not degrade oleanane-type saponins, i.e., soyasaponin Bb and glycyrrhizin; or the former sapogenin: soyasapogenol B (Fig. 2). Next, we assessed the time course of  $\alpha$ -tomatine degradation by RC1 (Fig. S2). With a reaction time of 90 min, RC1 degraded  $\alpha$ -tomatine into several products, including two peaks with retention times of 6.6 and 5.2 min, respectively. The former gave a major mass fragment ion at  $m/z$  416, identical to authentic tomatidine; whereas the latter exhibited a parental ion at  $m/z$  740 that was estimated to be  $\gamma$ -tomatine, in which one molecule each of D-glucose and D-xylose were removed from  $\alpha$ -tomatine. RC1 completely degraded  $\alpha$ -tomatine and its degradation intermediates within 180 min. Therefore, it was predicted that *Sphingobium* first hydrolyzes the oligosaccharide parts of steroid-type saponins in a stepwise manner, followed by sapogenin degradation.

### Selection of candidate genes responsible for saponin degradation via whole-genome analysis

We performed whole-genome sequencing of RC1 and 14 isolates from  $\alpha$ -tomatine-treated soils, to identify the genes involved in the degradation of steroid-type saponins in *Sphingobium*. The 16S rRNA V4 regions of all strains but TomTYG65, TomTYG72, TomTYG74, and TomMM15 were identical to those of the amplicon sequence variant (ASV) belonging to *Sphingobium*, which were remarkably increased by steroid-type saponins (28, 41) (Fig. S3). The total sequence length of all isolates ranged from 3.5 to 4.4 Mbp, which was comparable to that of closely related strains (Data Set S1). BUSCO assessments (42) classified all obtained genome assemblies as being of high quality (completeness score >99%) (Data Set S1). We searched for genes encoding steroid-type saponin degradation enzymes in the RC1 genome, from which 3,627 coding sequences (CDSs) were annotated using the Prokka pipeline (43) (Data Set S1).

### GHs for saponin degradation

A total of 33 glycoside hydrolases (GHs) were extracted from the RC1 genome and were classified into specific GH families using dbCAN2, which is a meta server for automated carbohydrate-active enzyme (CAZyme) annotation (44) (Data Set S2). In addition, we found that a total of six GH genes existed in close proximity in two regions of the RC1 genome and belonged to GH families 3, 39, 78, and 106 (Fig. S4). Glycoside hydrolases that cleave the glycoside bonds in ginsenosides, called ginsenosidases, have been identified from several microorganisms and belong to GH families 1, 2, 3, 10, 39, 42, 51, and 78 (45). The GH106 family from *Novosphingobium* sp. PP1Y reportedly exhibits rhamnosidase activity toward flavonoid glycosides (46). Therefore, we selected NNNEINPD\_01945, NNNEINPD\_01944, NNNEINPD\_01942, NNNEINPD\_03247, NNNEINPD\_03248, and NNNEINPD\_03250 as steroid-type saponin GH candidates, and termed them *SpGH3-4*, *SpGH39-1*, *SpGH3-3*, *SpGH3-1*, *SpGH106-1*, and *SpGH78-1*, respectively (Fig. S4).

Previously, tomatinases produced by tomato pathogens, such as *Fusarium oxysporum* f. sp. *lycopersici*, were shown to be extracellular enzymes that hydrolyze  $\alpha$ -tomatine by cleaving the glycoside bond (35). Our *in silico* analysis using SignalP 6.0, version 0.0.52 (47), strongly suggested that the six GH candidates contain signal peptides at their N termini. *SpGH3-1*, *SpGH78-1*, and *SpGH106-1* were predicted to have signal peptides for the general secretion protein export pathway, called Sec/SPI, whereas *SpGH3-3*, *SpGH3-4*, and *SpGH39-1* were predicted to have signal peptides for the twin-arginine translocation pathway, called Tat/SPI.

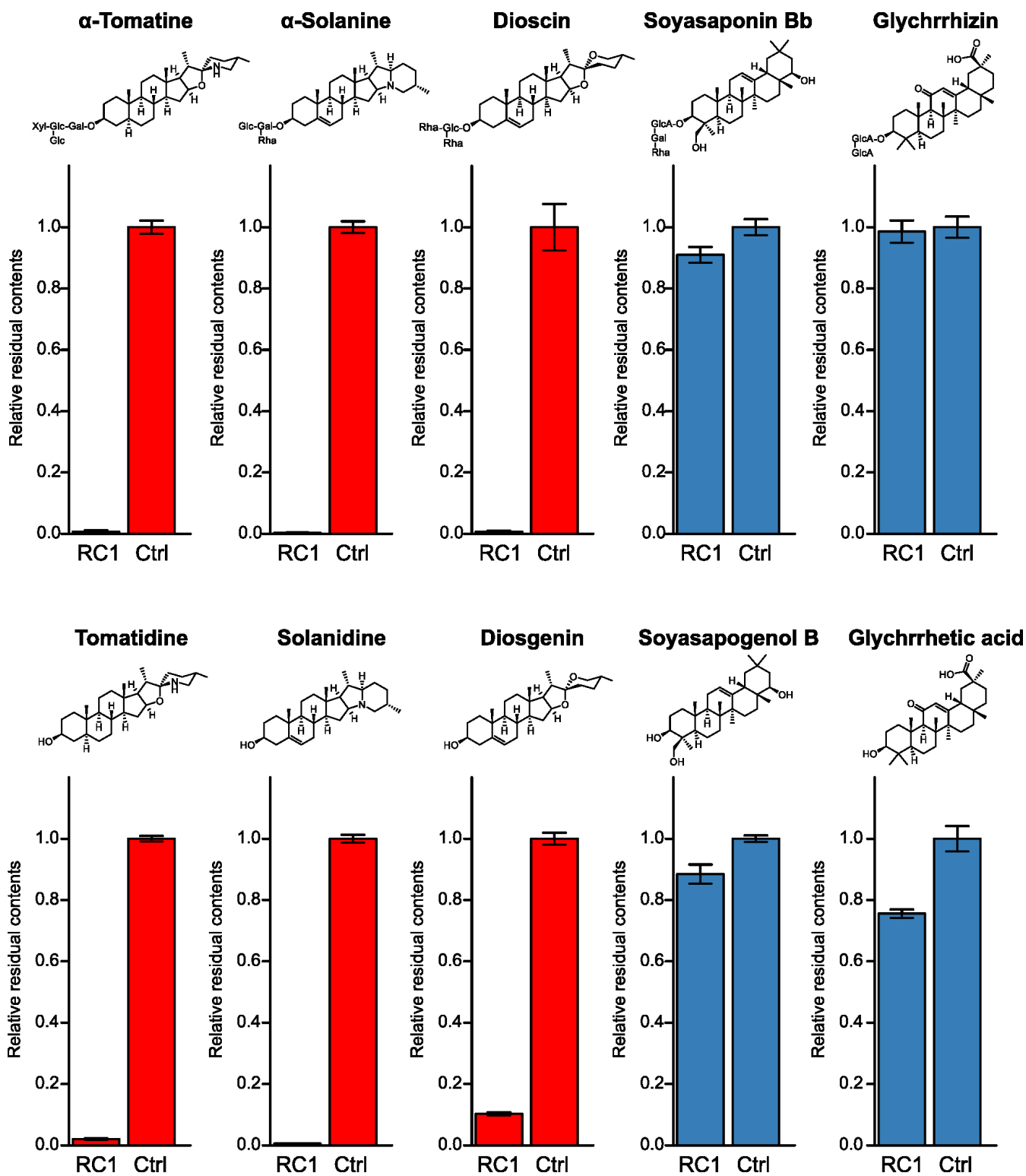


**FIG 2** Substrate specificity of the saponin- and sapogenin-degradation activities in RC1 resting cells. The residual substrate contents in the reaction mixture incubated for 3 h are shown relative to that obtained without RC1, as the negative control (Ctrl). The error bars indicate the standard deviation ( $n = 3$ , technical replicates).

## Enzymes for sapogenin degradation

We hypothesized that those orthologs of steroid degradation enzymes in RC1 are involved in the degradation of steroid-type sapogenins. Functional annotation using Kofam KOALA assigned several proteins of RC1 that were involved in the conversion of 5 $\alpha$ -androstane-3,17-dione and androst-5-en-3,17-dione to 4,5:9,10-diseco-3-hydroxy-5,9,17-trioxoandrost-1(10),2-diene-4-oate in the KEGG pathway map for steroid degradation (Fig. S5). This result indicated that RC1 carries a set of steroid degradation genes, which were predicted here to also participate in sapogenin degradation.

C3 oxidation is considered to be the initial reaction step in the microbial degradation of steroids with a hydroxyl group at the C-3 position. However, no RC1 proteins were assigned to this reaction in the KEGG pathway (Fig. S5). To identify the enzymes that are responsible for the initial reaction step of sapogenin degradation, we performed a BLAST search against all protein sequences in RC1 using the 3,17 $\beta$ -hydroxysteroid dehydrogenase (3,17 $\beta$ -HSD) encoded by the EGO55\_02230 gene in *N. tardaugens* ARI-1 as a query (40). NNNEINPD\_03057 and NNNEINPD\_02694 in RC1 exhibited 71% and 54% amino acid identities with EGO55\_02230, respectively, and shared 55% amino acid identity with each other. We selected NNNEINPD\_03057 and NNNEINPD\_02694 as candidates for sapogenin 3 $\beta$ -hydroxysteroid dehydrogenase (3 $\beta$ HSD), and designated them Sp3 $\beta$ HSD1 and Sp3 $\beta$ HSD2, respectively.

In steroid metabolism, the 3 $\beta$ HSDs in a wide range of organisms are often bifunctional enzymes that oxidize  $\Delta$ 5-3-hydroxysteroids at C3, to form  $\Delta$ 5-3-ketosteroids, then isomerize them to form  $\Delta$ 4-3-ketosteroids. In turn,  $\Delta$ 4-3-ketosteroids are also formed by 3-ketosteroid- $\Delta$ 4-dehydrogenase (3KS $\Delta$ 4DH), which catalyzes the  $\Delta$ 4-dehydrogenation of 3-ketosteroids containing a single bond between C5 and C6. A BLAST search showed that the 3KS $\Delta$ 4DH encoded by EGO55\_13615 in *N. tardaugens* ARI-1 (40) exhibited an amino acid identity of 46% with NNNEINPD\_01949 from RC1. The four 3KS $\Delta$ 4DH orthologs were assigned to the corresponding reaction in the KEGG pathway (Fig. S5). NNNEINPD\_01949 is located in the proximity of SpGH3-4, SpGH39-1, and SpGH3-3 in the RC1 genome. Therefore, we selected NNNEINPD\_01949 as the candidate enzyme for sapogenin degradation, and termed it Sp3KS $\Delta$ 4DH1.

## Comparative transcriptome analysis of $\alpha$ -tomatine-treated and mock-treated RC1

In several tomato pathogens, tomatinase activity and the expression of tomatinase genes have been reported to be induced by  $\alpha$ -tomatine treatment (37, 48, 49). We investigated whether an  $\alpha$ -tomatine-degrading activity was similarly induced in RC1. Treatment with  $\alpha$ -tomatine enhanced the degradation activity of RC1 cells (Fig. S6), suggesting that RC1 induces the expression of the degradation enzymes in response to saponin secretion by plants. A comparative transcriptome analysis between  $\alpha$ -tomatine-treated and mock-treated RC1 revealed that the transcript levels of the genes encoding the six saponin GH candidates, Sp3 $\beta$ HSD1, Sp3 $\beta$ HSD2, and six ortholog groups assigned to the steroid degradation pathway were expressed at higher levels in  $\alpha$ -tomatine-treated vs. mock-treated RC1 (Table S2). The increased expression of these genes in  $\alpha$ -tomatine-treated cells indicated that they were potential candidates for further characterization.

## In vitro functional analysis of steroid-type saponin GH candidates

To investigate the catalytic activities of steroid-type saponin GH candidates, the predicted mature forms of the candidates, in which the N-terminal predicted signal peptides were truncated, were expressed in *Escherichia coli*. The enzymatic activities of the candidates were examined using various saponins as substrates (Fig. 3; Fig. S7 and S8; Table S3).

The use of  $\alpha$ -tomatine as a substrate led to its conversion by SpGH3-4 to a product with a retention time of 19.4 min and a mass fragment ion at  $m/z$  902.5, which was

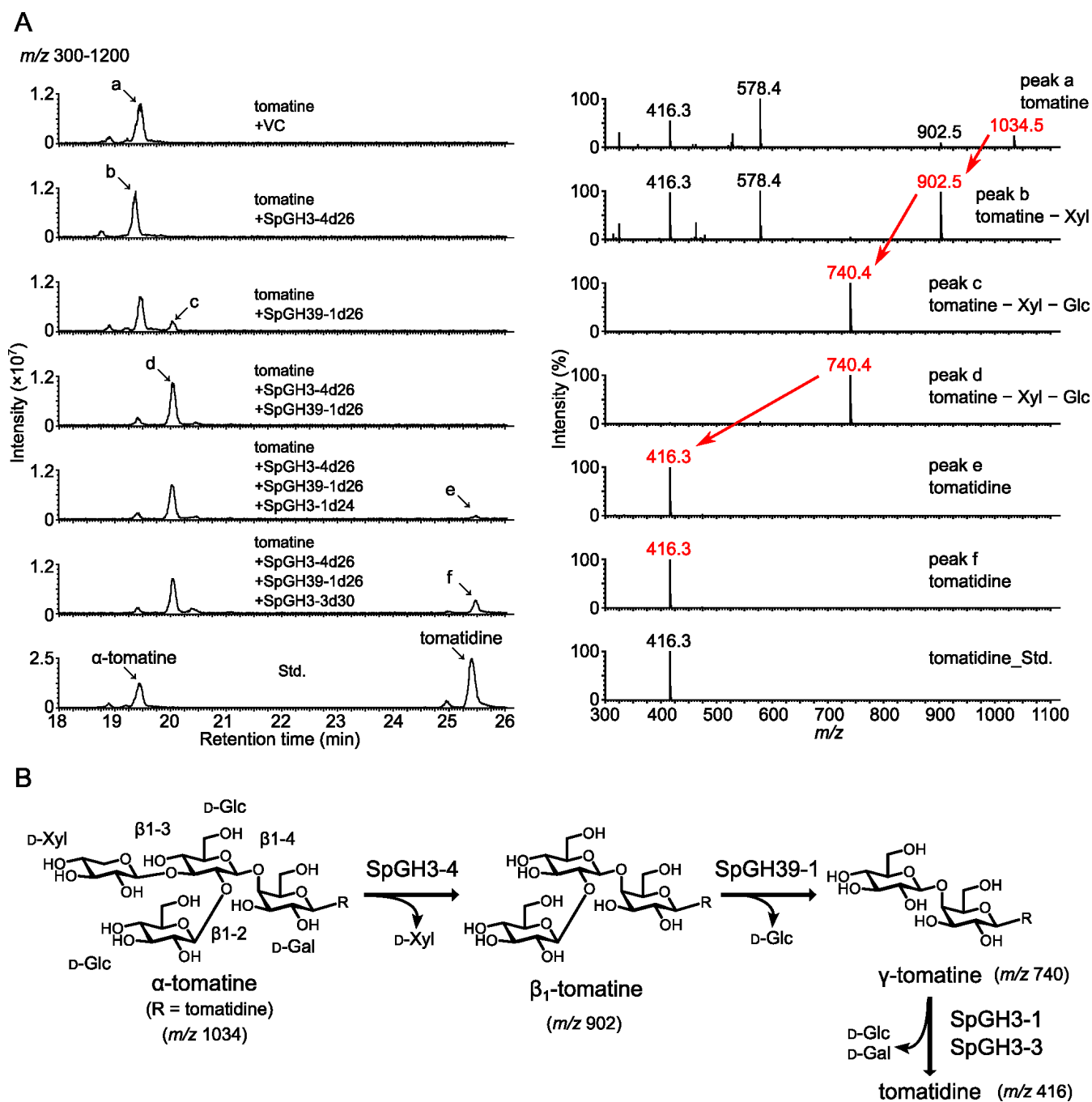


**FIG 3** Enzymatic activities of SpGH3-1, SpGH3-3, SpGH3-4, and SpGH39-1 toward  $\alpha$ -tomatine. (A) LC-MS analysis of the reaction products obtained from the recombinant proteins of SpGH3-1, SpGH3-3, SpGH3-4, and SpGH39-1 using  $\alpha$ -tomatine as a substrate. A purified protein from *Escherichia coli* transformed with an empty pET22b vector was used as the negative control (VC). Representative data of the enzymatic activities measured in biological duplicates are shown. The total ion current chromatogram obtained in the positive ionization mode with a full-scan range of  $m/z$  300–1200 is shown. The mass spectra of peak a (substrate,  $\alpha$ -tomatine) and peaks b–f (reaction products), and tomatidine standard, indicated by arrows in the chromatogram, are shown. The red letters represent the parental ion mass given by the reaction products. (B) Proposed enzymatic conversion of  $\alpha$ -tomatine to tomatidine, as predicted by the mass spectra of the reaction products.

132 mass smaller than that of  $\alpha$ -tomatine, suggestive of  $\beta_1$ -tomatine (Fig. 3A). Although incubation with SpGH39-1 left most of the  $\alpha$ -tomatine in the assay mixture, a reaction product detected at a retention time of 20.0 min gave a mass fragment ion at  $m/z$  740.4, which was 294 mass smaller than that of  $\alpha$ -tomatine, suggestive of  $\gamma$ -tomatine



(Fig. 3A). Moreover, coincubation with SpGH3-4 and SpGH39-1 metabolized most of  $\alpha$ -tomatine to  $\gamma$ -tomatine (Fig. 3A). These results indicate that SpGH3-4 hydrolyzed the  $\beta$ 1–3 linked  $D$ -xylose from  $\alpha$ -tomatine, to produce  $\beta$ 1-tomatine, and that SpGH39-1 mainly hydrolyzed the  $\beta$ 1–2 linked  $D$ -glucose from  $\beta$ 1-tomatine, to produce  $\gamma$ -tomatine (Fig. 3B). Furthermore, coincubation of SpGH3-1 with SpGH3-4 and SpGH39-1 gave a peak with a retention time of 25.5 min and a mass fragment ion at  $m/z$  416.3, which was found to be identical to that of tomatidine (Fig. 3A). Finally, coincubation of SpGH3-3 with SpGH3-4 and SpGH39-1 also yielded tomatidine (Fig. 3A). These results suggest that SpGH3-1 and SpGH3-3 hydrolyzed the  $\beta$ - $D$ -glucosyl-(1 $\rightarrow$ 4)- $\beta$ - $D$ -galactosyl moiety from  $\gamma$ -tomatine to produce tomatidine (Fig. 3B).

We next measured the enzymatic activities of GH candidates using other saponins as substrates. In brief, SpGH106-1 hydrolyzed  $\alpha$ 1-2 linked  $L$ -rhamnose from  $\alpha$ -solanine (Fig. S7B), whereas SpGH3-1 and SpGH3-3 hydrolyzed  $\beta$ 1-3 linked  $D$ -glucose from  $\beta$ 2-solanine and then  $D$ -galactose from  $\gamma$ -solanine, to eventually produce solanidine (Fig. S7B). SpGH106-1 and SpGH78-1 probably hydrolyzed  $\alpha$ 1-2- and  $\alpha$ 1-4-linked  $L$ -rhamnose from dioscin, respectively, and SpGH3-1 subsequently hydrolyzed  $D$ -glucose from diosgenin-3- $O$ - $\beta$ - $D$ -glucoside, to produce diosgenin (Fig. S8B).

The use of soyasaponin Bb and glycyrrhizin as substrates did not yield any product peaks from the six saponin GH candidates, indicating that they are specific GHs for steroid-type saponins (Table S3). Moreover, SpGH3-4 and SpGH39-1 did not recognize  $\alpha$ -solanine and dioscin as substrates, and SpGH78-1 and SpGH106-1 did not metabolize  $\alpha$ -tomatine (Table S3).

### ***In vitro* functional analysis of Sp3 $\beta$ HSD1, Sp3 $\beta$ HSD2, and Sp3KSD4DH1 toward pregnane derivatives and sapogenins**

Recombinant proteins of Sp3 $\beta$ HSD1, Sp3 $\beta$ HSD2, and Sp3KSD4DH1 were prepared using a bacterial expression system in *E. coli*, for use in *in vitro* assays. First, their enzymatic activities were analyzed using pregnane derivatives as substrates (Fig. S9 to S11). Sp3 $\beta$ HSD1 and Sp3 $\beta$ HSD2 converted isopregnanolone to a product with a retention time of 11.2 min and a major mass fragment ion at  $m/z$  317.3, which was identical to that of 5 $\alpha$ -pregnane-3,20-dione (Fig. S9). Subsequently, they also converted pregnenolone to a product with a retention time of 10.2 min and a major mass fragment ion at  $m/z$  315.3, which was identical to that of progesterone (Fig. S10). Sp3KSD4DH1 metabolized 5 $\alpha$ -pregnane-3,20-dione to a product with a retention time of 10.2 min and a major mass fragment ion at  $m/z$  315.3, which was identical to that of progesterone (Fig. S11). These results indicated that Sp3 $\beta$ HSD1 and Sp3 $\beta$ HSD2 catalyzed the C3 oxidation and  $\Delta$ 5- $\Delta$ 4 isomerization of pregnane derivatives, and that Sp3KSD4DH1 catalyzed their  $\Delta$ 4-dehydrogenation.

Next, the enzymatic activities of Sp3 $\beta$ HSD1, Sp3 $\beta$ HSD2, and Sp3KSD4DH1 toward several sapogenins were surveyed (Fig. 4; Fig. S12 to S15). The use of tomatidine as a substrate led to a reaction product from Sp3 $\beta$ HSD1 and Sp3 $\beta$ HSD2 with a retention time of 10.0 min and a major mass fragment ion at  $m/z$  414.3, which was two mass smaller than that of tomatidine (used as the substrate) (Fig. 4A). In turn, coincubation of Sp3KSD4DH1 with either Sp3 $\beta$ HSD1 or Sp3 $\beta$ HSD2 produced a peak with a retention time of 9.0 min and a major mass fragment ion at  $m/z$  412.3, which was four mass smaller than that of tomatidine (Fig. 4A). Based on their enzymatic activities toward pregnane derivatives, it was suggested that Sp3 $\beta$ HSD1 and Sp3 $\beta$ HSD2 converted tomatidine to tomatid-3-one, which was then metabolized to tomatid-4-en-3-one by Sp3KSD4DH1 (Fig. 4B). Similarly, using solanidine, diosgenin, and glycyrrhetic acid as substrates, Sp3 $\beta$ HSD1 and Sp3 $\beta$ HSD2 produced peaks with major mass fragment ions that were two mass smaller than their respective substrates (Fig. S12 to S14). These results suggest that Sp3 $\beta$ HSD1 and Sp3 $\beta$ HSD2 converted solanidine, diosgenin, and glycyrrhetic acid to solanid-4-en-3-one, diosgen-4-en-3-one, and 3-keto-glycyrrhetic acid, respectively. In contrast, soyasapogenol B was not recognized as a substrate for Sp3 $\beta$ HSD1 and Sp3 $\beta$ HSD2 (Fig. S15).

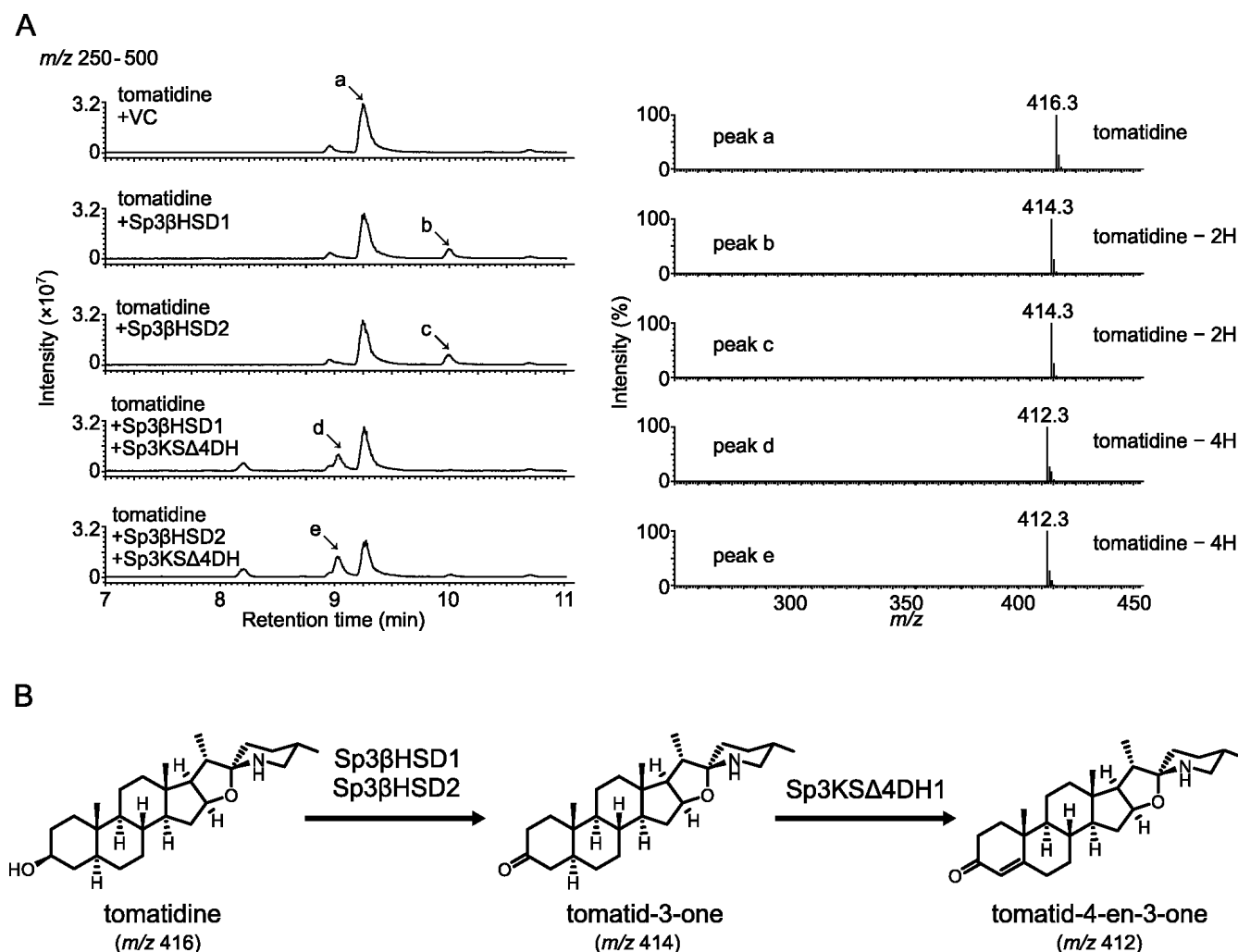


**FIG 4** Enzymatic activities of Sp3 $\beta$ HSD1, Sp3 $\beta$ HSD2, and Sp3KSD4DH1 toward tomatidine. (A) LC-MS analysis of the reaction products obtained from the recombinant proteins of Sp3 $\beta$ HSD1, Sp3 $\beta$ HSD2, and Sp3KSD4DH1 using tomatidine as a substrate. A purified protein from *Escherichia coli* transformed with an empty pET22b vector was used as the negative control (VC). Representative data of the enzymatic activities measured in biological duplicates are shown. The total ion current chromatogram obtained in the positive ionization mode with a full-scan range of  $m/z$  250–500 is shown. The mass spectra of peak a (substrate, tomatidine) and peaks b–e (reaction products), as indicated by arrows in the chromatogram, are shown. (B) Proposed enzymatic conversion of tomatidine to tomatid-4-en-3-one, as predicted by the enzymatic activities of Sp3 $\beta$ HSD1 and Sp3 $\beta$ HSD2 toward isopregnanolone (Fig. S9) and of Sp3KSD4DH1 toward 5 $\alpha$ -pregnane-3,20-dione (Fig. S11).

### Distribution of the genes encoding steroid-catabolizing enzymes and saponin GHs in *Sphingobium* spp.

We identified several steroid-catabolizing enzymes and saponin GHs in RC1. Subsequently, we investigated whether the genes encoding these enzymes were present in the genus *Sphingobium*, including other  $\alpha$ -tomatine-degrading isolates. We performed a comparative genomic analysis between 15 of our isolates and 34 strains that have whole-genome sequences that are registered in public databases (Fig. 5; Data Set S4). A phylogenetic tree constructed based on core genes showed that our  $\alpha$ -tomatine-degrading isolates were located in a specific clade (Fig. 5). All  $\alpha$ -tomatine-degrading isolates possessed a set of homologous genes encoding Sp3 $\beta$ HSD2, steroid-catabolizing enzymes, and six saponin GHs (Fig. 5). Unlike Sp3 $\beta$ HSD2, Sp3 $\beta$ HSD1 was absent in TomTYG74, TomTYG65, and TomMM35A; however, this probably did not affect the degradation of relevant saponins because of complementation by Sp3 $\beta$ HSD2 (Fig. 5). Regarding the strains from the public database, GCF\_001658005.1 possessed the

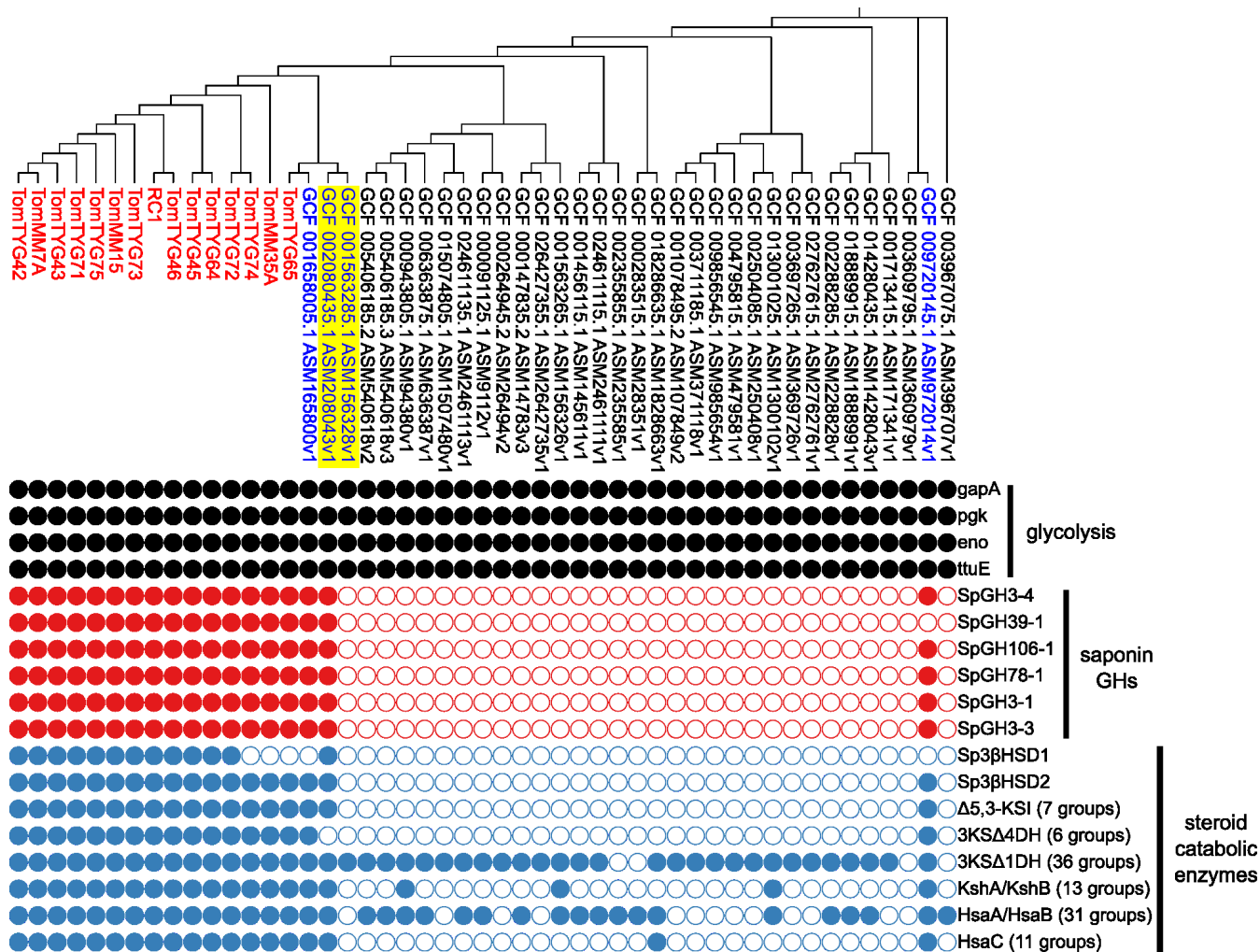


**FIG 5** Phylogenetic distribution of the genes encoding saponin glycoside hydrolases (GHs) and steroid-catabolizing enzymes in *Spingobium* spp. including  $\alpha$ -tomatine-degrading isolates. Gene presence and absence are indicated by closed and open circles, respectively. The number of groups in parentheses represents the number of groups of orthologous genes (OGs) annotated for each enzyme, and enzymes with at least one OG are indicated by closed circles. The red and blue letters indicate our isolates and strains from the public database mentioned in this article, respectively. GCF\_002080435.1 ASM208043v1 and GCF\_001563285.1 ASM156328v1 highlighted in yellow correspond to NBRC16415 and JCM17233 in Fig. 6, respectively.

gene set described above, with the exception of *Sp3βHSD1*, suggesting that it can completely degrade steroid-type saponins (Fig. 5). In contrast, because *3KSD4DH* and *SpGH39-1* were absent in GCF\_002080435.1 and GCF\_009720145.1, respectively, the two strains may partially degrade steroid-type saponins and then accumulate the precursors for each enzyme as the degradation intermediates (Fig. 5). The strains from the public database, with the exception of GCF\_001658005.1, GCF\_002080435.1, and GCF\_009720145.1, did not possess saponin GHs or most of the steroid-catabolizing enzymes, suggesting that they are unable to degrade steroid-type saponins (Fig. 5).

Next, we measured the degradation activities of two *Spingobium* strains, *S. herbicidovorans* MH (NBRC16415) and *Spingobium* sp. MI1205 (JCM17233), corresponding to GCF\_002080435.1 and GCF\_001563285.1, respectively (Fig. 6), which were closely related to each other (Fig. 5). Incubation of their resting cells with  $\alpha$ -tomatine showed that NBRC16415, which carried a gene set that excluded *3KSD4DH*, degraded this compound and produced two peaks with retention times of 5.7 and 5.4 min and major mass fragment ions at  $m/z$  410 and  $m/z$  408, respectively (Fig. 6), which were thought to be putative degradation intermediates. In contrast, JCM17233, which carried only

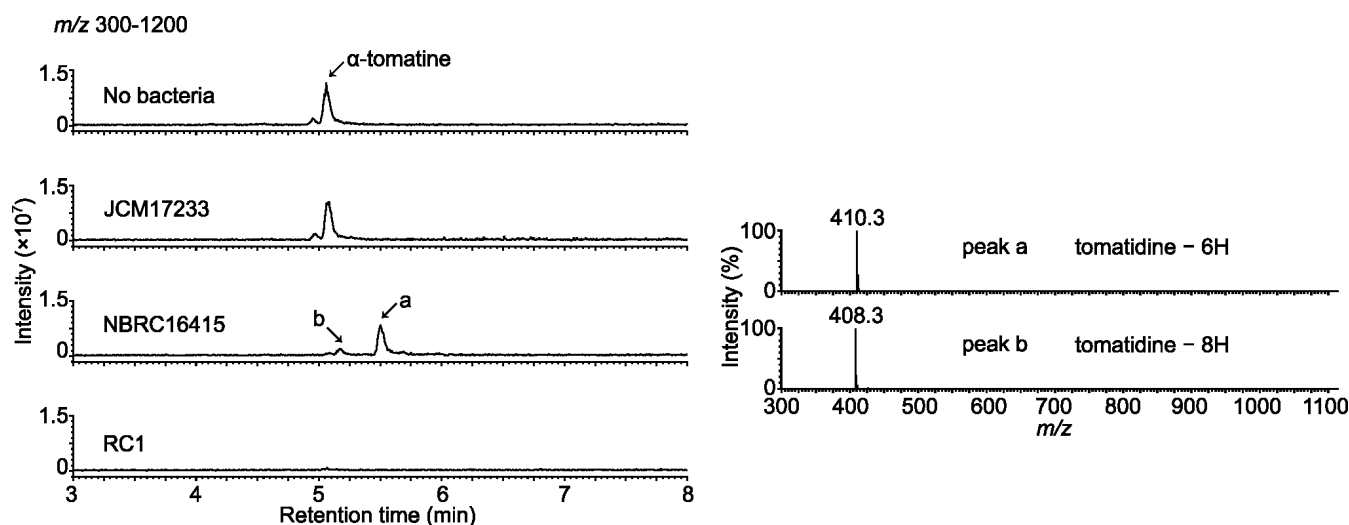


**FIG 6**  $\alpha$ -Tomatine-degradation activities in three *Sphingobium* strains, JCM17233, NBRC16415, and RC1. LC-MS analysis of the reaction products obtained from the respective resting cells incubated for 24 h using  $\alpha$ -tomatine as a substrate. A reaction mixture without cells was used as the negative control (no bacteria). Representative data of the degradation activities measured in technical triplicates are shown. The total ion current chromatogram obtained in the positive ionization mode with a full-scan range of  $m/z$  300–1200 is shown. The mass spectra of peaks a and b (reaction products), as indicated by arrows in the chromatogram, are shown. NBRC16415 and JCM17233 correspond to GCF 002080435.1 ASM208043v1 and GCF 001563285.1 ASM156328v1 in Fig. 5, respectively.

*3KSD1DH* in its genome, did not degrade  $\alpha$ -tomatine (Fig. 6). These results revealed that the presence of genes encoding degradative enzymes was consistent with the degradation activities of saponins.

## DISCUSSION

In this study, we identified the enzymes that were responsible for the degradation of  $\alpha$ -tomatine and related steroidal saponins in *Sphingobium* sp. RC1, which was isolated from tomato roots. SpGH3-4, SpGH39-1, and SpGH3-1/-3 coordinately degraded  $\alpha$ -tomatine to tomatidine. The reported GH3 hydroxylase family of microbial saponin degradation enzymes exhibits 1,2-, 1-4-, and 1-6- $\beta$ -D-glucosidase and 1-6- $\alpha$ -L-arabinopyranosidase activities (34, 36, 50–52). Avenacinase in the oat fungal pathogen *Gaeumannomyces graminis* var. *avenae* removes the terminal  $\beta$ -1,2- and  $\beta$ -1,4-linked D-glucose molecules from avenacin A-1 (34). In turn, tomatinase of the tomato pathogen *Septoria lycopersici* removes the terminal  $\beta$ -1,2-linked D-glucose from  $\alpha$ -tomatine, which is named  $\beta_2$ -tomatinase because it yields  $\beta_2$ -tomatine as the reaction product (36). Although the two GHs specifically recognize their respective host saponins as substrates, both GHs belong to the GH3 family and have 1,2- $\beta$ -D-glucosidase activity for their substrates (50). GH3 enzymes with other activities, for example 1,6- $\beta$ -D-glucosidase and 1-6- $\alpha$ -L-arabinopyranosidase activities, have also been identified as ginsenosidases in several microorganisms (51, 52). Here, none of the GH3 enzymes tested in *Sphingobium* sp. RC1 exhibited 1,2- $\beta$ -D-glucosidase activity toward  $\alpha$ -tomatine, whereas SpGH3-1, SpGH3-3, and SpGH3-4 displayed different activities (Fig. 3; Fig. S7 and S8). These findings indicated that microbial saponin-hydrolyzing GH3 enzymes possess diverse substrate specificities and regioselectivities.

Alternatively, a gene product detected in RC1, SpGH39-1, catalyzed 1,2- $\beta$ -D-glucosidase activity toward  $\beta_1$ -tomatine. Thus, it may have acted as a multifunctional enzyme that removed both  $\beta$ -1,2-D-glucose and  $\beta$ -1,3-D-xylose from  $\alpha$ -tomatine, to produce  $\gamma$ -tomatine (Fig. 3). Most of the bacterial GH39 enzymes characterized to date exhibit  $\beta$ -xylosidase activity (53). The GH39 enzymes in *Thermoanaerobacterium thermosaccharolyticum* and *Sphingomonas* sp. JB13 have been identified as ginsenosidases that hydrolyze the C-6 outer  $\beta$ -1,2-D-xylosidic linkage (54, 55). In contrast, a GH39 enzyme in *Croceicoccus marinus* E4A9 (CmGH1) had  $\beta$ -glucosidase activity, instead of  $\beta$ -D-xylosidase

activity (56). Future biochemical analyses of GH39 enzymes, including SpGH39-1, will provide new insights into their multifunctional catalytic mechanism.

GH78 enzymes are found in bacteria and fungi, whereas GH106 enzymes are found exclusively in bacteria. All characterized enzymes in both families predominantly exhibited  $\alpha$ -L-rhamnosidase activities. SpGH106-1 and SpGH78-1 showed putative 1,2- and 1,4- $\alpha$ -L-rhamnosidase activities toward steroidal saponins, respectively (Fig. S7 and S8). A GH78 enzyme present in the *Absidia* sp. 39 fungal strain has been identified as a ginsenosidase that hydrolyzes the C-6 outer  $\alpha$ -1,2-L-rhamnosidic linkage (57). Recently, in two bacterial strains, i.e., *Arthrobacter* sp. S41 from soils surrounding green potato peels and *Glutamicibacter halophytocola* S2 from the gut of a potato pest (*Phthorimaea operculella*), three GHs belonging to the GH2, GH3, and GH78 families, respectively, were reported to exist as the gene cluster in respective genomes and to catalyze the complete deglycosylation of both  $\alpha$ -chaconine and  $\alpha$ -solanine (58, 59). All three GHs from the latter strain have been characterized as multifunctional enzymes that cleave multiple types of glycosidic bonds (59). In contrast, SpGH78-1 did not recognize  $\alpha$ -solanine as a substrate (Table S3), indicating that its enzymatic properties are different from those of the GH78 enzymes characterized previously. A GH106 enzyme responsible for saponin degradation has not been identified to date. Therefore, SpGH106-1 was an enzyme with saponin-hydrolyzing ability that was unique in this family.

Microbial steroid-degrading enzymes have been well studied in several soil-borne microorganisms, and degradation pathways have been proposed (39). Metagenomics analyses of the genes encoding steroid-catabolizing enzymes from various environments revealed that those isolated from Alphaproteobacteria and Actinobacteria are predominant in the rhizosphere, and that the former mainly consist of *Sphingomonadaceae* and Rhizobiales (60). In general, plants produce a complex mixture of sterols, which are a subgroup of steroids that serve as integral components of the lipid bilayer of biological membranes and the precursors of plant hormones in the brassinosteroid class (61, 62), implying that the ability of those microbial taxa to degrade steroids contributes to their utilization as nutrients and colonization in the plant rhizosphere. Accordingly, several strains of *Mycobacteria* and *Rhodococcus* from Actinobacteria and *Novosphingobium* and *Sphingomonas* from *Sphingomonadaceae* can degrade steroids, such as cholesterol, cholic acids, androgens, estrogens, and their derivatives, to use them as energy sources (63–66). The early steps of steroid degradation, i.e., C3 oxidation and C1,4-desaturation (67), have also been observed in tomatidine modification by *Nocardia* and *Arthrobacter* of Actinobacteria, which convert it into tomatid-4-en-3-one (68, 69). Here, Sp3 $\beta$ HSD1 and Sp3 $\beta$ HSD2 of *Sphingobium* sp. RC1, which are the orthologs of steroid-degrading enzymes, metabolized tomatidine, solanidine, and diosgenin to produce peaks with mass fragments corresponding to their respective putative 4-en-3-one derivatives (Fig. 4; Fig. S12 and S13). Based on the known steroid degradation pathway (Fig. S5), we proposed a putative tomatidine degradation pathway in RC1 (Fig. S16). The identification of the enzymes that catalyze the first step of sapogenin degradation may pave the way toward the characterization of the saponin degradation pathway in soil bacteria, because we can postulate that orthologous genes to the steroid degradation pathway are involved in the sapogenin degradation pathway. This was supported by our observation that NBRC16415, with a gene set that excluded 3KSD4DH, did not completely degrade tomatidine and metabolized  $\alpha$ -tomatine to putative degradation intermediates (Fig. 6).

The enzymatic degradation of saponins contributes to the pathogenesis of various microorganisms. For instance, oat, tomato, and potato pathogens produce GHs termed avenacinase, tomatinase, and  $\alpha$ -chaconinase, which remove the sugar moiety from the avenacin A-1,  $\alpha$ -tomatine, and  $\alpha$ -chaconine accumulated in each host plant, respectively (34–38). Avenacinase-deficient mutants of the oat fungal pathogen *Gaeumannomyces graminis* var. *avenae* are unable to infect oats (70). Moreover, the heterologous expression of the tomatinase gene from the tomato fungal pathogen *Septoria lycopersici* in another tomato fungal pathogen (*Cladosporium fulvum*) enhanced its virulence toward tomato, and a tomatinase-deficient mutant of *C. fulvum* exhibited reduced virulence (49,

71). Accordingly, the RC1  $\alpha$ -tomatine-degrading enzymes identified in this study may also be involved in interactions with tomato plants.

Our comparative genomics analysis revealed that the orthologs of the degradation enzymes were present not only in our  $\alpha$ -tomatine-degrading isolates belonging to a phylogenetically specific clade of *Sphingobium*, but also in GCF\_009720145.1, which is phylogenetically distant from them (Fig. 5). In the RC1 genome, *SpGH3-4*, *SpGH39-1*, and *SpGH3-3* were present in a chromosome, whereas *SpGH3-1*, *SpGH106-1*, and *SpGH78-1* were located in a plasmid (Fig. S4). These data imply that both vertical (inherited from a common ancestor) and horizontal (transferred from a phylogenetically unrelated organism of the same generation) gene transmission events resulted in the acquisition of the genes encoding degradation enzymes in some strains of *Sphingobium*. This was consistent with the presence of genomic features in *Arthrobacter*, in which catabolic genes for nicotine and santhopine, which are PSMs secreted from tobacco roots, indicate their transfer in both vertical and horizontal manners (72). Because bacterial isolates that metabolize PSMs are isolated from the rhizosphere of the plant species that accumulate these PSMs (73, 74), we proposed that the catabolic abilities of *Arthrobacter* are associated with their ability to colonize tobacco roots (72). These observations support the hypothesis that the genes involved in saponin degradation in tomato-root-associated *Sphingobium* strains provide them with a survival advantage in the presence of bioactive saponins in the tomato rhizosphere.

## MATERIALS AND METHODS

### Chemicals, plant materials, bacterial strains, and soils

$\alpha$ -Tomatine, diosgenin, glycyrrhizin, glycyrrhetic acid, pregnenolone, 5 $\alpha$ -pregnane-3,20-dione, and progesterone were purchased from Tokyo Chemical Industry Co., Ltd. (Tokyo, Japan). Tomatidine and dioscin were purchased from Cayman Chemical (Ann Arbor, MI, USA), and 2,6-dichlorophenol indophenol (DCPIP) and  $\beta$ -nicotinamide-adenine dinucleotide oxidized form ( $\beta$ -NAD<sup>+</sup>) were purchased from Nakalai Tesque, Inc. (Kyoto, Japan).  $\alpha$ -Solanine, solanidine, a mixture of soyasaponin from soybeans (mainly soyasaponin Bb), soyasapogenol B, and isopregnanolone were purchased from Extrasynthese (Genay, France), Sigma-Aldrich (St. Louis, MO, USA), FUJIFILM Wako Pure Chemical Corporation (Osaka, Japan), Tokiwa Phytochemical (Chiba, Japan), and Santa Cruz Biotechnology (Dallas, TX, USA), respectively. Seeds of tomato (*S. lycopersicum*) cv. Benisuzume were purchased from the Institute for Horticultural Plant Breeding (Chiba, Japan). The bacterial strains used in this study are listed in Table S1. The *S. herbicidovorans* MH (NBRC16415) and *Sphingobium* sp. MI1205 (JCM17233) strains were provided by the Biological Resource Center, NITE (NBRC) (Chiba, Japan) and Japan Collection of Microorganisms, RIKEN BRC (Ibaraki, Japan) through the National BioResource Project of the MEXT, respectively. Field soils were sampled at the field of the Kyoto University of Advanced Science (KUAS), Kameoka, Kyoto, Japan (34°59'37.7"N, 135°33'05.0"E), air dried, and sieved as described in our previous study (75).

### Cultivation of field-grown tomato plants and sampling of their roots

Tomato seeds were sown in pots filled with a 1:1 mixture of vermiculite and field soils. Seedlings were grown in the laboratory for 4 weeks at 25°C under a 16-h light/8-h dark cycle, and then in a greenhouse for 10 weeks. They were planted in the field of KUAS on 12 June 2020. The roots of the tomato plants were sampled at the flowering stage on 9 July 2020. They were kept cool using an ice pack and transported to the laboratory. The rhizosphere and rhizoplane soils were removed from the roots via gentle shaking for 5 min and sonication for 5 min in phosphate-buffered saline (PBS; pH 7.0) containing 130 mM NaCl, 7 mM Na<sub>2</sub>HPO<sub>4</sub>, 3 mM NaH<sub>2</sub>PO<sub>4</sub>, and 0.02% Silwet L-77 (76). After rinsing with tap water, the endosphere compartments were stored at 4°C until bacteria were isolated (one overnight).

## Isolation of *Shingobium* spp. from $\alpha$ -tomatine-treated soils and field-grown tomato plants

The isolation of bacterial strains from  $\alpha$ -tomatine-treated soils was carried out as described in our previous work (28), with minor modifications. Briefly, the soil suspensions diluted with sterile water were distributed onto agar plates prepared using tryptone yeast extract glucose (TYG) medium (77), in addition to mineral salt buffer (MS) medium (78) containing 20  $\mu\text{g mL}^{-1}$  of  $\alpha$ -tomatine or tomatidine as the sole carbon source. To isolate tomato-root-inhabiting bacteria, 1 g of the endosphere compartments was homogenized with a mortar and pestle in 10 mL of 10 mM  $\text{MgCl}_2$  solution and distributed onto TYG agar plates. All plates were incubated for up to 7 days at 28°C. Yellow colonies were picked up from the plates, and their genomic DNA was extracted using the hot-alkaline DNA extraction method; each colony was suspended in 10  $\mu\text{L}$  of a buffer containing 25 mM NaOH and 0.2 mM EDTA and incubated at 95°C for 30 min, followed by the addition of 10  $\mu\text{L}$  of 40 mM Tris-HCl solution (pH 6.8). Using these DNA extracts as templates, the 16S rRNA genes in the respective isolates were PCR amplified using KOD FX Neo (TOYOBO, Osaka, Japan) and the primer set: 10F (5'-GTTTGATCCTGGCTCA-3') and 800R (5'-TACCAGGGTATCTAATCC-3'). The PCR conditions were as follows: 94°C for 2 min; followed by 35 cycles at 98°C for 10 s, 50°C for 30 s, and 68°C for 1 min. The PCR products were purified using a Wizard Genomic DNA Purification Kit (Promega, Madison, WI, USA), according to the manufacturer's instructions, and sequenced using the 10F primer. ClustalW was used to align the obtained 16S rRNA V4 region. Bacterial isolates that were annotated as *Shingobium* spp. by a BLAST search were cultured in a growth medium (pH 7.0) containing 10 g  $\text{L}^{-1}$  peptone, 10 g  $\text{L}^{-1}$  beef extract, and 5 g  $\text{L}^{-1}$  NaCl, and then stored in a 20% glycerol solution at  $-80^\circ\text{C}$ .

### Genomic DNA extraction, whole-genome sequencing, and annotation

Each stock culture of bacterial isolates was streaked onto the agar plates. A single colony was pre-cultured in 2 mL of the growth medium and further cultivated in 10 mL of the same medium for 2 days at 28°C, respectively. The culture was harvested by centrifugation at  $4,000 \times g$  for 5 min. The cell pellets were washed with 5 mL of TE buffer consisting of 10 mM Tris-HCl (pH 8.0) and 1 mM EDTA, and stored at  $-30^\circ\text{C}$  until genomic DNA extraction. Genomic DNA was extracted as described previously, with modifications (79). The cell pellets were lysed in 600  $\mu\text{L}$  of TE buffer containing 20 mg  $\text{mL}^{-1}$  lysozyme and incubated for 30 min at 37°C. Fifty microliter of 20% (wt/vol) sodium dodecyl sulfate in aqueous solution and 25  $\mu\text{L}$  of TE buffer containing 20 mg  $\text{mL}^{-1}$  proteinase K were added to the cells, followed by incubation for 30 min at 37°C. The cleared lysate was forced through a syringe (38  $\times$  0.8 mm) 10 times, and proteins were removed using the TE-saturated phenol:chloroform:isoamyl alcohol (25:24:1) method. The genomic DNA was collected using the ethanol precipitation method and dissolved in 100  $\mu\text{L}$  of TE buffer. The DNA concentration was measured using a BioSpec-nano instrument (Shimadzu, Kyoto, Japan) and a Qubit 2.0 Fluorometer (Thermo Fisher Scientific, Waltham, MA, USA).

Library construction and whole-genome sequencing were performed as described previously, with minor modifications (72). Briefly, a DNA library was cut off at 15 kbp using the Blue Pippin size-selection system (Sage Science, Beverly, MA, USA). Genomes were assembled using the Hierarchical Genome Assembly Process v.4 within SMRTlink (v.10.0 for RC1; v.8.0 for the remaining strains), and exhibited the expected size. Circlator v.1.5.5 (80) was used to evaluate whether the genome assemblies were circularizable and to predict the location of the starting position.

The obtained genomes were automatically annotated using the Prokka pipeline, to predict CDSs, tRNAs, and rRNAs (43). The completeness and redundancy of genomic data were evaluated via the assignment of the protein sequences in each isolate to the sphingomonadales\_odb10 data set using BUSCO, version v5.4.4 (42). KEGG orthologs were assigned to proteins in RC1 using Kofam KOALA (81). Finally, CAZymes (including

GHs) in RC1 were extracted from the RC1 total proteins using dbCAN2 with default parameters (44).

### Measurements of the saponin- and sapogenin-degrading activities using resting cells

The saponin- and sapogenin-degrading activities of the bacterial strains were measured using their resting cells. Each strain was cultivated in 2 mL of the growth medium for 2 days, followed by centrifugation of the culture at  $4,000 \times g$  for 5 min. Cell pellets were washed twice with 1 mL of MS medium and then resuspended to  $OD_{600} = 2.0$  using the same medium. A resting cell reaction was performed in 100  $\mu$ L of MS medium including 20  $\mu$ M each substrate and cell suspensions at  $OD_{600} = 1.0$ . The reaction was carried out at 28°C for 3 or 24 h, and stopped using 100  $\mu$ L of methanol. The reaction mixture was centrifuged at  $10,000 \times g$  for 1 min, filtered through a 0.45  $\mu$ m Minisart RC4 filter (Sartorius, Göttingen, Germany), and applied to LC-MS analysis.

### Heterologous expression of recombinant proteins in *E. coli*

The coding sequences of saponin-degrading candidate genes were PCR amplified using the RC1 genomic DNA as a template, which was extracted using the hot-alkaline DNA extraction method described above with the primer sets listed on Data Set S3. The amplified DNA fragments were ligated into the pGEM-T Easy Vector (Promega). The DNA fragments of CDS were ligated into pET22b (Merck KGaA, Darmstadt, Germany) using restriction enzymes or an In-Fusion HD Cloning Kit (Takara Bio, Shiga, Japan). In addition, the CDSs of *Sp3KSD4DH1* were codon-optimized for *E. coli* expression using the Codon Optimization Tool (ExpOptimizer) (<https://novoprolabs.com/tools/codon> optimization) provided by NovoPro Inc. (Shanghai, China). The codon-optimized sequences with a TIR-2 sequence located upstream, which is a promoter that can increase the protein-production yield in *E. coli* (82), were synthesized and inserted into pET28a by Twist Bioscience (South San Francisco, CA, USA). *E. coli* strain BL21 (DE3) (Takara Bio) was transformed with the constructed vector and grown at 37°C in 50 mL of lysogeny broth containing 50  $\mu$ g mL<sup>-1</sup> ampicillin until its  $OD_{600}$  reached 0.5. Recombinant protein expression was induced by adding isopropyl  $\beta$ -D-1-thiogalactopyranoside at a final concentration of 100  $\mu$ M and was continued for 20 h at 18°C. The culture was harvested by centrifugation at  $10,000 \times g$  for 5 min at 4°C. The cell pellets were washed twice with cold PBS buffer and stored at -30°C until the *in vitro* assay. Each cell pellet was resuspended in 1 mL of a cold lysis buffer consisting of 50 mM sodium phosphate (pH 8.0), 300 mM NaCl, and 10 mM imidazole; followed by five rounds of sonication for 15 s using an ultrasonic homogenizer (Sonifier Model 250A; Branson, Danbury, CT, USA) with the following settings: a duty cycle of 50% and an output control of 20%. The homogenate was centrifuged at  $10,000 \times g$  for 5 min at 4°C, and the supernatant was used for the purification of His-tagged proteins. One hundred and fifty microliters of Ni-NTA agarose (QIAGEN) were loaded onto Micro Bio-Spin Chromatography Columns (bed volume, 0.8 mL) (Bio-Rad, Hercules, CA, USA). The resin was equilibrated with 600  $\mu$ L of the lysis buffer and centrifuged at  $1,000 \times g$  for 1 min at 4°C, to remove the buffer. His-tagged proteins in 600  $\mu$ L of the supernatant were bound to the Ni-NTA resin and washed twice with 600  $\mu$ L of a wash buffer consisting of 50 mM sodium phosphate (pH 8.0), 300 mM NaCl, and 20 mM imidazole. The adsorbed proteins were eluted twice with 100  $\mu$ L of an elution buffer consisting of 50 mM sodium phosphate (pH 8.0), 300 mM NaCl, and 250 mM imidazole. The concentration of the purified recombinant proteins was measured using a Qubit 2.0 Fluorometer and were used in *in vitro* assays.

### Measurements of saponin- and sapogenin-degrading activities using recombinant proteins

An *in vitro* assay of recombinant Sp3 $\beta$ HSD1 and Sp3 $\beta$ HSD2 was performed using 100  $\mu$ L of a reaction mixture consisting of 50 mM sodium phosphate (pH 7.0), 1 mM  $\beta$ -NAD<sup>+</sup>



(as a coenzyme), 50  $\mu\text{M}$  sapogenins and pregnane derivatives (as substrates), and 1  $\mu\text{g}$  of each recombinant protein. The enzymatic activities of Sp3KS $\Delta$ 4DH1 were measured by adding 1  $\mu\text{g}$  of each recombinant protein to the reaction mixtures described above. For the latter, 1 mM DCPIP was added as an electron acceptor. An *in vitro* assay of recombinant GHs was performed using 100  $\mu\text{L}$  of a reaction mixture consisting of 50 mM potassium phosphate (pH 6.0), 50  $\mu\text{M}$  saponins (as substrates), and 1  $\mu\text{g}$  of the respective recombinant proteins. All reactions were carried out at 37°C for 2 h, and then stopped by adding 100  $\mu\text{L}$  of *n*-butanol saturated with water. The reaction mixture was extracted three times by vortexing and centrifugation at 10,000  $\times g$  for 1 min. The organic phase was collected and dried *in vacuo*. The residue was dissolved in 200  $\mu\text{L}$  of methanol, filtered through a 0.45- $\mu\text{m}$  Minisart RC4 filter (Sartorius), and applied to LC-MS analysis.

### LC-MS analysis of reaction products using resting cells and recombinant proteins

The microbial and enzymatic reaction products were analyzed using an Acquity ultra-high-performance liquid chromatography (UPLC) HClass/Xevo TQD instrument (Waters). For each sample, 2  $\mu\text{L}$  was injected into an Acquity UPLC HSS T3 column (1.7  $\mu\text{m}$ ; 2.1  $\times$  100 mm<sup>2</sup>; Waters) using a UPLC HSS T3 VanGuard Precolumn (1.7  $\mu\text{m}$ , 2.1  $\times$  5 mm<sup>2</sup>) or an Acquity UPLC BEH C18 column (1.7  $\mu\text{m}$ , 2.1  $\times$  50 mm<sup>2</sup>; Waters) with an UPLC BEH C18 VanGuard Precolumn (1.7  $\mu\text{m}$ ; 2.1  $\times$  5 mm<sup>2</sup>). The former was used for the analysis of the reaction products from resting cells of *Sphingobium* isolates with  $\alpha$ -tomatine (Fig. S1), followed by recombinant GHs with  $\alpha$ -tomatine and  $\alpha$ -solanine (Fig. S7 and S8); whereas the latter was used for the remaining ones. The column oven temperature was set at 40°C. The mobile phases consisted in water containing 0.1% (vol/vol) formic acid (solvent A) and acetonitrile (solvent B). The flow rate was set at 0.2 mL min<sup>-1</sup>. The mass spectra were obtained in the positive electrospray ionization mode using following settings: cone voltage of 30 V; capillary voltage of 3.15 kV; source temperature of 150°C; desolvation gas temperature of 400°C; nebulizer and desolvation N<sub>2</sub> gas flow rates of 50 and 800 L h<sup>-1</sup>, respectively. The elution programs and mass conditions used for each analysis are described in Text S1. The data obtained were analyzed using the MassLynx v. 4.1 software (Waters).

### Comparative genomic analysis of *Sphingobium* spp.

A comparative genomic analysis of *Sphingobium* spp. was performed on our isolates and on with complete genome sequences that were registered in NCBI database, as listed in Data Set S4. Their coding sequences, which were annotated by the Prokka pipeline, as described above, were used to cluster orthologous genes (OGs) via the Roary v3.13.0 pipeline with a minimum percentage identity of 75% for BLASTP (83). Genes that were present in 95% or more of the strains were defined as core genes. All core genes were aligned using MAFFT (84), and the alignment was employed to build a phylogenetic tree using FastTree (85). The binary matrix with presence and absence of genes across all strains was used to draw the phylogenetic distribution of metabolic genes using Interactive Tree Of Life (iTOL), which is an online tool for the display, manipulation, and annotation of phylogenetic trees (86).

### Total RNA extraction, RNA-seq, and transcriptome analysis

RC1 cell suspensions at OD<sub>600</sub> = 0.5 in MS medium (7.5 mL) were treated with 75  $\mu\text{L}$  of 5 mM  $\alpha$ -tomatine dissolved in methanol. An equal volume of methanol was used as the mock treatment. Both  $\alpha$ -tomatine- and mock-treatments were performed in technical duplicates. After incubation at 28°C for 3 h, 1 mL of the suspension was centrifuged at 10,000  $\times g$  for 1 min, and cell pellets were stored at -80°C until total RNA extraction. The residual suspension was used to investigate the induction of  $\alpha$ -tomatine-degrading activity by  $\alpha$ -tomatine treatment. The resting cells were prepared as a substrate as described in the "Measurements of the saponin- and sapogenin-degrading activities

using resting cells" subsection. The resting cell reaction was performed in 1 mL of MS medium consisting of 50  $\mu$ M  $\alpha$ -tomatine and cell suspensions at  $OD_{600} = 0.5$ . After 1, 2, and 3 h from the start of the reaction, 100  $\mu$ L of each of the suspensions was collected and mixed with an equal volume of methanol and applied to LC-MS analysis, as described above.

Total RNA was extracted from RC1 cells treated with  $\alpha$ -tomatine using the TRI reagent (Cosmo Bio Co., Ltd., Tokyo, Japan), according to the manufacturer's instructions. The RNA concentration was measured using a Qubit 2.0 Fluorometer. The total RNA library was prepared using the TruSeq stranded total RNA library (bacteria) (Illumina, San Diego, CA, USA) and applied to  $2 \times 100$  bp paired-end sequencing on a NovaSeq6000 platform (Illumina) at Macrogen Japan Corp. (Tokyo, Japan). The paired-end reads were used to quantify the abundances of transcripts with CDSs of RC1 (as a reference) using Kallisto version 0.46.2 (87), which is an RNA-seq quantification program, with default parameters. The obtained Kallisto pseudo-counts (TPM) are listed in Table S2 and Data Set S5.

## ACKNOWLEDGMENTS

We would like to thank Ms. Rie Mizuno for technical assistance; Dr. Hisabumi Takase and Dr. Jiro Sekiya for providing soil samples and supporting our field experiment; Dr. Tomohisa Shimasaki for helpful discussion; Dr. Ryosuke Munakata, Dr. Tomohisa Shimasaki, Ms. Hinako Matsuda, and Mr. Noritaka Aoki for the critical reading of the manuscript; and DASH/FBAS, the Research Institute for Sustainable Humanosphere, Kyoto University, for supporting institutional setting.

This study was supported in part by grants from the Core Research for Evolutional Science and Technology, Japan Science and Technology Agency (CREST, JST; JPMJCR17O2 to Y.A. and A. Sugiyama); Japan Society for the Promotion of Science KAKENHI (21H02329 to A. Sugiyama, 20H05592 to S.M., 20H05909 and 22H00364 to K.S.); and the Research Institute for Sustainable Humanosphere (Mission 1) to A. Sugiyama.

M.N. and A. Sugiyama conceived and designed the research. K.Y. and A. Sugiyama supervised the experiments. M.N., K.T., and A. Sugiyama cultivated tomato plants at the field and sampled them. M.N. and K.K. isolated bacterial strains. M.N., S.M., A. Shibata., W.S., and K.S. conducted whole-genome sequencing. M.N., S.Y., and Y.A. analyzed the bacterial genome data. M.N. performed RNA-seq experiments and transcriptome analysis. M.N., K.T., and K.K. measured of the enzymatic activities using resting cells and recombinant proteins. M.N., S.M., and A. Sugiyama wrote the article with contributions of all the authors. M.N. and A. Sugiyama agree to serve as the authors responsible for contact and ensure communication.

We declare no competing interests.

## AUTHOR AFFILIATIONS

<sup>1</sup>Research Institute for Sustainable Humanosphere, Kyoto University, Uji, Kyoto, Japan

<sup>2</sup>Plant Immunity Research Group, RIKEN Center for Sustainable Resource Science, Yokohama, Kanagawa, Japan

<sup>3</sup>Tohoku Medical Megabank Organization, Tohoku University, Sendai, Miyagi, Japan

<sup>4</sup>Graduate School of Information Sciences, Tohoku University, Sendai, Miyagi, Japan

<sup>5</sup>Laboratory for Microbiome Sciences, RIKEN Center for Integrative Medical Sciences, Yokohama, Kanagawa, Japan

## AUTHOR ORCIDs

Kyoko Takamatsu  <http://orcid.org/0000-0002-3961-4339>

Akifumi Sugiyama  <http://orcid.org/0000-0002-9643-6639>

## FUNDING

Funder	Grant(s)	Author(s)
MEXT   JST   Core Research for Evolutional Science and Technology (CREST)	JPMJCR17O2	Akifumi Sugiyama
MEXT   JST   Core Research for Evolutional Science and Technology (CREST)	JPMJCR17O2	Yuichi Aoki
MEXT   Japan Society for the Promotion of Science (JSPS)	21H02329	Akifumi Sugiyama
MEXT   Japan Society for the Promotion of Science (JSPS)	20H05592	Sachiko Masuda
MEXT   Japan Society for the Promotion of Science (JSPS)	20H05909	Ken Shirasu
MEXT   Japan Society for the Promotion of Science (JSPS)	22H00364	Ken Shirasu

## DATA AVAILABILITY

The acquired sequence data sets that supported the conclusions of this study were registered in the DNA Data Bank of Japan (DDBJ) Sequence Read Archive (accession numbers: [DRA015721](#) and [DRA015722](#) for the whole-genome sequencing of *Sphingobium* isolates and transcriptome of RC1, respectively). The nucleotide sequences of *SpGH3-1*, *SpGH3-3*, *SpGH3-4*, *SpGH39-1*, *SpGH78-1*, *SpGH106-1*, *Sp3βHSD1*, *Sp3βHSD2*, and *Sp3KSD4DH1*, which were identified in this study, were registered to DDBJ (accession numbers: [LC754524](#), [LC754525](#), [LC754526](#), [LC754527](#), [LC754528](#), [LC754529](#), [LC754530](#), [LC754531](#), and [LC754532](#), respectively).

## ADDITIONAL FILES

The following material is available [online](#).

### Supplemental Material

**DATA SET S1 (mBio00599-23-s0001.xlsx)**. Assembly results of the *Sphingobium* isolates used in this study.

**DATA SET S2 (mBio00599-23-s0002.xlsx)**. List of the RC1 glycoside hydrolase genes annotated using dbCAN2.

**DATA SET S3 (mBio00599-23-s0003.xlsx)**. Primer sequences used in this study.

**DATA SET S4 (mBio00599-23-s0004.xlsx)**. Public genome assembly used in the comparative genomic analysis.

**DATA SET S5 (mBio00599-23-s0005.xlsx)**. The transcript levels of all genes in α-tomatine- and mock-treated RC1 cells.

**TEXT S1 (mBio00599-23-s0006.docx)**. Elution programs and mass conditions for detection of each reaction product in LC-MS analysis.

**Supplemental Material (mBio00599-23-s0007.pdf)**. Fig. S1 to S16; Tables S1 to S3.

## REFERENCES

- Hartmann A, Rothballer M, Schmid M. 2008. Lorenz Hiltner, a pioneer in rhizosphere microbial ecology and soil bacteriology research. *Plant Soil* 312:7–14. <https://doi.org/10.1007/s11104-007-9514-z>
- Guerrieri A, Dong LM, Bouwmeester HJ. 2019. Role and exploitation of underground chemical signaling in plants. *Pest Manag Sci* 75:2455–2463. <https://doi.org/10.1002/ps.5507>
- Massalha H, Korenblum E, Tholl D, Aharoni A. 2017. Small molecules below-ground: the role of specialized metabolites in the rhizosphere. *Plant J* 90:788–807. <https://doi.org/10.1111/tpj.13543>
- Pascale A, Proietti S, Pantelides IS, Stringlis IA. 2019. Modulation of the root microbiome by plant molecules: the basis for targeted disease suppression and plant growth promotion. *Front Plant Sci* 10:1741. <https://doi.org/10.3389/fpls.2019.01741>
- Jacoby RP, Koprivova A, Kopriva S. 2021. Pinpointing secondary metabolites that shape the composition and function of the plant microbiome. *J Exp Bot* 72:57–69. <https://doi.org/10.1093/jxb/eraa424>
- Sugiyama A. 2021. Flavonoids and saponins in plant rhizospheres: roles, dynamics, and the potential for agriculture. *Biosci Biotechnol Biochem* 85:1919–1931. <https://doi.org/10.1093/bbb/zbab106>
- Harbort CJ, Hashimoto M, Inoue H, Niu Y, Guan R, Rombolà AD, Kopriva S, Voges M, Sattely ES, Garrido-Oter R, Schulze-Lefert P. 2020. Root-secreted coumarins and the microbiota interact to improve iron

- nutrition in Arabidopsis. *Cell Host Microbe* 28:825–837. <https://doi.org/10.1016/j.chom.2020.09.006>
8. Hu L, Robert CAM, Cadot S, Zhang X, Ye M, Li B, Manzo D, Chervet N, Steinger T, van der Heijden MGA, Schlaeppi K, Erb M. 2018. Root exudate metabolites drive plant-soil feedbacks on growth and defense by shaping the rhizosphere microbiota. *Nat Commun* 9:13. <https://doi.org/10.1038/s41467-018-05122-7>
  9. Yu P, He X, Baer M, Beirinckx S, Tian T, Moya YAT, Zhang X, Deichmann M, Frey FP, Bresgen V, Li C, Razavi BS, Schaaf G, von Wirén N, Su Z, Bucher M, Tsuda K, Goormachtig S, Chen X, Hochholdinger F. 2021. Plant flavones enrich rhizosphere *Oxalobacteraceae* to improve maize performance under nitrogen deprivation. *Nat Plants* 7:481–499. <https://doi.org/10.1038/s41477-021-00897-y>
  10. Zhong Y, Xun WB, Wang XH, Tian SW, Zhang YC, Li DW, Zhou Y, Qin YX, Zhang B, Zhao GW, Cheng X, Liu YG, Chen HM, Li LG, Osbourn A, Lucas WJ, Huang SW, Ma YS, Shang Y. 2022. Root-secreted bitter triterpene modulates the rhizosphere microbiota to improve plant fitness. *Nat Plants* 8:887–896. <https://doi.org/10.1038/s41477-022-01201-2>
  11. He D, Singh SK, Peng L, Kaushal R, Vílchez JI, Shao C, Wu X, Zheng S, Morcillo RJL, Paré PW, Zhang H. 2022. Flavonoid-attracted *Aeromonas* sp. from the Arabidopsis root microbiome enhances plant dehydration resistance. *ISME J* 16:2622–2632. <https://doi.org/10.1038/s41396-022-01288-7>
  12. Sparg SG, Light ME, van Staden J. 2004. Biological activities and distribution of plant saponins. *J Ethnopharmacol* 94:219–243. <https://doi.org/10.1016/j.jep.2004.05.016>
  13. Moses T, Papadopoulou KK, Osbourn A. 2014. Metabolic and functional diversity of saponins, biosynthetic intermediates and semi-synthetic derivatives. *Crit Rev Biochem Mol Biol* 49:439–462. <https://doi.org/10.3109/10409238.2014.953628>
  14. Cárdenas PD, Almeida A, Bak S. 2019. Evolution of structural diversity of triterpenoids. *Front Plant Sci* 10:1523. <https://doi.org/10.3389/fpls.2019.01523>
  15. Miettinen K, Iñigo S, Kreft L, Pollier J, De Bo C, Botzki A, Coppens F, Bak S, Goossens A. 2018. The TriForC database: a comprehensive up-to-date resource of plant triterpene biosynthesis. *Nucleic Acids Res* 46:D586–D594. <https://doi.org/10.1093/nar/gkx925>
  16. Kitagawa I. 2002. Licorice root. A-natural sweetener and an important ingredient in Chinese medicine. *Pure and Applied Chemistry* 74:1189–1198. <https://doi.org/10.1351/pac200274071189>
  17. Sautour M, Mitaine-Offer AC, Lacaille-Dubois MA. 2007. The *Dioscorea* genus: a review of bioactive steroid saponins. *J Nat Med* 61:91–101. <https://doi.org/10.1007/s11418-006-0126-3>
  18. Friedman M. 2002. Tomato glycoalkaloids: role in the plant and in the diet. *J Agric Food Chem* 50:5751–5780. <https://doi.org/10.1021/jf020560c>
  19. Friedman M. 2006. Potato glycoalkaloids and metabolites: roles in the plant and in the diet. *J Agric Food Chem* 54:8655–8681. <https://doi.org/10.1021/jf061471t>
  20. Vincken J-P, Heng L, de Groot A, Gruppen H. 2007. Saponins, classification and occurrence in the plant kingdom. *Phytochemistry* 68:275–297. <https://doi.org/10.1016/j.phytochem.2006.10.008>
  21. Oleszek W, Jurzysta M, Gorski P. 1992. Alfalfa saponins—the allelopathic agents, p 151–167. In *Allelopathy: basic and applied aspects*: <https://doi.org/10.1007/978-94-011-2376-1>
  22. Faizal A, Geelen D. 2013. Saponins and their role in biological processes in plants. *Phytochem Rev* 12:877–893. <https://doi.org/10.1007/s11101-013-9322-4>
  23. Hussain M, Debnath B, Qasim M, Bamsile BS, Islam W, Hameed MS, Wang L, Qiu D. 2019. Role of saponins in plant defense against specialist herbivores. *Molecules* 24:2067. <https://doi.org/10.3390/molecules24112067>
  24. Nakayasu M, Shiota N, Shikata M, Thagun C, Abdelkareem A, Okabe Y, Ariizumi T, Arimura G-I, Mizutani M, Ezura H, Hashimoto T, Shoji T. 2018. JRE4 is a master transcriptional regulator of defense-related steroidal glycoalkaloids in tomato. *Plant J* 94:975–990. <https://doi.org/10.1111/tpj.13911>
  25. Papadopoulou K, Melton RE, Leggett M, Daniels MJ, Osbourn AE. 1999. Compromised disease resistance in saponin-deficient plants. *Proc Natl Acad Sci U S A* 96:12923–12928. <https://doi.org/10.1073/pnas.96.22.12923>
  26. Tsuno Y, Fujimatsu T, Endo K, Sugiyama A, Yazaki K. 2018. Soyasaponins: a new class of root exudates in soybean (*Glycine max*). *Plant Cell Physiol* 59:366–375. <https://doi.org/10.1093/pcp/pcx192>
  27. Fujimatsu T, Endo K, Yazaki K, Sugiyama A. 2020. Secretion dynamics of soyasaponins in soybean roots and effects to modify the bacterial composition. *Plant Direct* 4:e00259. <https://doi.org/10.1002/pld3.259>
  28. Nakayasu M, Ohno K, Takamatsu K, Aoki Y, Yamazaki S, Takase H, Shoji T, Yazaki K, Sugiyama A. 2021. Tomato roots secrete tomatine to modulate the bacterial assemblage of the rhizosphere. *Plant Physiol* 186:270–284. <https://doi.org/10.1093/plphys/kiab069>
  29. Nakayasu M, Takamatsu K, Yazaki K, Sugiyama A. 2022. Plant specialized metabolites in the rhizosphere of tomatoes: secretion and effects on microorganisms. *Biosci Biotechnol Biochem* 87:13–20. <https://doi.org/10.1093/mbb/zbac181>
  30. Hennessy RC, Jørgensen NOG, Scavenius C, Enghild JJ, Greve-Poulsen M, Sørensen OB, Stougaard P. 2018. A screening method for the isolation of bacteria capable of degrading toxic steroidal glycoalkaloids present in potato. *Front Microbiol* 9:2648. <https://doi.org/10.3389/fmicb.2018.02648>
  31. Navarro del Hierro J, Herrera T, Fornari T, Reglero G, Martin D. 2018. The gastrointestinal behavior of saponins and its significance for their bioavailability and bioactivities. *J Func Foods* 40:484–497. <https://doi.org/10.1016/j.jff.2017.11.032>
  32. He Y, Hu Z, Li A, Zhu Z, Yang N, Ying Z, He J, Wang C, Yin S, Cheng S. 2019. Recent advances in biotransformation of saponins. *Molecules* 24:2365. <https://doi.org/10.3390/molecules24132365>
  33. Zhang S, Shu J, Xue H, Zhang W, Zhang Y, Liu Y, Fang L, Wang Y, Wang H, Heck M. 2020. The gut microbiota in camellia weevils are influenced by plant secondary metabolites and contribute to saponin degradation. *mSystems* 5:e00692-19. <https://doi.org/10.1128/mSystems.00692-19>
  34. Osbourn AE, Clarke BR, Dow JM, Daniels MJ. 1991. Partial characterization of avenacinase from *Gaeumannomyces-graminis* VAR avenae. *Physiol Mol Plant Pathol* 38:301–312. [https://doi.org/10.1016/S0885-5765\(05\)80121-3](https://doi.org/10.1016/S0885-5765(05)80121-3)
  35. Lairini K, Perez-Espinosa A, Pineda M, Ruiz-Rubio M. 1996. Purification and characterization of tomatinase from *Fusarium oxysporum* f sp lycopersici. *Appl Environ Microbiol* 62:1604–1609. <https://doi.org/10.1128/aem.62.5.1604-1609.1996>
  36. Sandrock RW, DellaPenna D, VanEtten HD. 1995. Purification and characterization of Beta<sub>2</sub>-tomatinase, an enzyme involved in the degradation of alpha-tomatine and isolation of the gene encoding Beta<sub>2</sub>-tomatinase from *Septoria lycopersici*. *Mol Plant Microbe Interact* 8:960–970. <https://doi.org/10.1094/mpmi-8-0960>
  37. Quidde T, Osbourn AE, Tudzynski P. 1998. Detoxification of α-tomatine by *Botrytis cinerea*. *Physiol Mol Plant Pathol* 52:151–165. <https://doi.org/10.1006/pmpp.1998.0142>
  38. Becker P, Weltring KM. 1998. Purification and characterization of α-chaconinase of *Gibberella pulicaris*. *FEMS Microbiol Lett* 167:197–202. <https://doi.org/10.1111/j.1574-6968.1998.tb13228.x>
  39. Horinouchi M, Koshino H, Malon M, Hirota H, Hayashi T. 2019. Steroid degradation in comamonas testosteroni TA441: identification of the entire β-oxidation cycle of the cleaved B ring. *Appl Environ Microbiol* 85:e01204-19. <https://doi.org/10.1128/AEM.01204-19>
  40. Ibero J, Galán B, Díaz E, García JL. 2019. Testosterone degradative pathway of *Novosphingobium tardaugens* Genes 10:871. <https://doi.org/10.3390/genes10110871>
  41. Nakayasu M, Ikeda K, Yamazaki S, Aoki Y, Yazaki K, Washida H, Sugiyama A. 2021. Two distinct soil disinfections differently modify the bacterial communities in a tomato field. *Agronomy* 11:1375. <https://doi.org/10.3390/agronomy11071375>
  42. Manni M, Berkeley MR, Seppey M, Simão FA, Zdobnov EM. 2021. BUSCO update: novel and streamlined workflows along with broader and deeper phylogenetic coverage for scoring of eukaryotic, prokaryotic, and viral genomes. *Mol Biol Evol* 38:4647–4654. <https://doi.org/10.1093/molbev/msab199>
  43. Seemann T. 2014. Prokka: rapid prokaryotic genome annotation. *Bioinformatics* 30:2068–2069. <https://doi.org/10.1093/bioinformatics/btu153>
  44. Zhang H, Yohe T, Huang L, Entwistle S, Wu P, Yang Z, Busk PK, Xu Y, Yin Y. 2018. dbCAN2: a meta server for automated carbohydrate-active

- enzyme annotation. *Nucleic Acids Res* 46:W95–W101. <https://doi.org/10.1093/nar/gky418>
45. Shin KC, Oh DK. 2016. Classification of glycosidases that hydrolyze the specific positions and types of sugar moieties in ginsenosides. *Crit Rev Biotechnol* 36:1036–1049. <https://doi.org/10.3109/07388551.2015.1083942>
  46. Mensitieri F, De Lise F, Strazzulli A, Moracci M, Notomista E, Cafaro V, Bedini E, Sazinsky MH, Trifuoggi M, Di Donato A, Izzo V. 2018. Structural and functional insights into RHA-P, a bacterial GH106  $\alpha$ -L-rhamnosidase from *Novosphingobium* sp. PP1Y. *Arch Biochem Biophys* 648:1–11. <https://doi.org/10.1016/j.abb.2018.04.013>
  47. Teufel F, Almagro Armenteros JJ, Johansen AR, Gíslason MH, Pihl SI, Tsigos KD, Winther O, Brunak S, von Heijne G, Nielsen H. 2022. Signalp 6.0 predicts all five types of signal peptides using protein language models. *Nat Biotechnol* 40:1023–1025. <https://doi.org/10.1038/s41587-021-01156-3>
  48. Roldán-Arjona T, Pérez-Espinosa A, Ruiz-Rubio M. 1999. Tomatinase from *Fusarium oxysporum* f. sp. lycopersici defines a new class of saponinases. *Mol Plant Microbe Interact* 12:852–861. <https://doi.org/10.1094/MPMI.1999.12.10.852>
  49. Ökmen B, Etalo DW, Joosten M, Bouwmeester HJ, de Vos RCH, Collemare J, de Wit P. 2013. Detoxification of  $\alpha$ -tomatine by *Cladosporium fulvum* is required for full virulence on tomato. *New Phytol* 198:1203–1214. <https://doi.org/10.1111/nph.12208>
  50. Osbourn A, Bowyer P, Lunness P, Clarke B, Daniels M. 1995. Fungal pathogens of oat roots and tomato leaves employ closely related enzymes to detoxify different host plant saponins. *Mol Plant Microbe Interact* 8:971–978. <https://doi.org/10.1094/mpmi-8-0971>
  51. Hong H, Cui CH, Kim JK, Jin FX, Kim SC, Im WT. 2012. Enzymatic biotransformation of ginsenoside RB1 and gypenoside XVII into ginsenosides RD and F2 by recombinant  $\beta$ -glucosidase from *Flavobacterium johnsoniae*. *J Ginseng Res* 36:418–424. <https://doi.org/10.5142/jgr.2012.36.4.418>
  52. Lee JH, Hyun Y-J, Kim D-H. 2011. Cloning and characterization of  $\alpha$ -L-arabinofuranosidase and bifunctional  $\alpha$ -L-arabinopyranosidase/ $\beta$ -D-galactopyranosidase from *Bifidobacterium longum* H-1. *J Appl Microbiol* 111:1097–1107. <https://doi.org/10.1111/j.1365-2672.2011.05128.x>
  53. Abbott W, Alber O, Bayer E, Berrin JG, Boraston A, Brumer H, Brzezinski R, Clarke A, Cobucci-Ponzano B, Cockburn D, Coutinho P, Czjzek M, Dassa B, Davies GJ, Eijsink V, Eklof J, Felice A, Ficko-Blean E, Pincher G, Fontaine T, Fujimoto Z, Fujita K, Fushinobu S, Gilbert H, Gloster T, Goddard-Borger E, Greig I, Hehemann JH, Hemsworth G, Henrissat B, Hidaka M, Hurtado-Guerrero R, Igarashi K, Ishida T, Janacek S, Jongkees S, Juge N, Kaneko S, Katayama T, Kitaoka M, Konno N, Kracher D, Kulminkskaya A, Bueren AL, Larsen S, Lee J, Linder M, LoLeggio L, Ludwig R, Luis A. 2018. Ten years of CAZypedia: a living encyclopedia of carbohydrate-active enzymes. *Glycobiology* 28:3–8. <https://doi.org/10.1093/glycob/cwx089>
  54. Shin KC, Seo MJ, Oh DK. 2014. Characterization of  $\beta$ -xylosidase from thermoanaerobacterium thermosaccharolyticum and its application to the production of ginsenosides RG(1) and RH-1 from notoginsenosides R-1 and R-2. *Biotechnol Lett* 36:2275–2281. <https://doi.org/10.1007/s10529-014-1604-4>
  55. Zhang R, Li N, Xu SJ, Han XW, Li CY, Wei X, Liu Y, Tu T, Tang XH, Zhou JP, Huang ZX. 2019. Glycoside hydrolase family 39  $\beta$ -xylosidases exhibit  $\beta$ -1,2-xylosidase activity for transformation of notoginsenosides: a new EC subclass. *J Agric Food Chem* 67:3220–3228. <https://doi.org/10.1021/acs.jafc.9b00027>
  56. Shen YF, Li ZY, Huo YY, Bao LY, Gao BC, Xiao P, Hu XJ, Xu XW, Li JX. 2019. Structural and functional insights into CmGH1, a novel GH39 family  $\beta$ -glucosidase from deep-sea bacterium. *Front Microbiol* 10:2922. <https://doi.org/10.3389/fmicb.2019.02922>
  57. Yu HS, Gong JM, Zhang CZ, Jin FX. 2002. Purification and characterization of ginsenoside- $\alpha$ -L-rhamnosidase. *Chem Pharm Bull (Tokyo)* 50:175–178. <https://doi.org/10.1248/cpb.50.175>
  58. Hennessy RC, Nielsen SD, Greve-Poulsen M, Larsen LB, Sørensen OB, Stougaard P. 2020. Discovery of a bacterial gene cluster for deglycosylation of toxic potato steroidal glycoalkaloids  $\alpha$ -chaconine and  $\alpha$ -solanine. *J Agric Food Chem* 68:1390–1396. <https://doi.org/10.1021/acs.jafc.9b07632>
  59. Wang WQ, Du GZ, Yang GY, Zhang K, Chen B, Xiao GL. 2022. A multifunctional enzyme portfolio for  $\alpha$ -chaconine and  $\alpha$ -solanine degradation in the *Phthorimaea operculella* gut bacterium *Glutamicibacter halophytocola* S2 encoded in a trisaccharide utilization locus. *Front Microbiol* 13. <https://doi.org/10.3389/fmicb.2022.1023698>
  60. Holert J, Cardenas E, Bergstrand LH, Zaikova E, Hahn AS, Hallam SJ, Mohn WW. 2018. Metagenomes reveal global distribution of bacterial steroid catabolism in natural, engineered, and host environments. *mBio* 9:e02345-17. <https://doi.org/10.1128/mBio.02345-17>
  61. Benveniste P. 2004. Biosynthesis and accumulation of sterols. *Annu Rev Plant Biol* 55:429–457. <https://doi.org/10.1146/annurev.arplant.55.031903.141616>
  62. Schaller H. 2004. New aspects of Sterol biosynthesis in growth and development of higher plants. *Plant Physiol Biochem* 42:465–476. <https://doi.org/10.1016/j.plaphy.2004.05.012>
  63. Fujii K, Satomi M, Morita N, Motomura T, Tanaka T, Kikuchi S. 2003. *Novosphingobium tardaugens* sp nov., an oestradiol-degrading bacterium isolated from activated sludge of a sewage treatment plant in Tokyo. *Int J Syst Evol Microbiol* 53:47–52. <https://doi.org/10.1099/ijs.0.02301-0>
  64. van Der Geize R, Hessels GI, van Gerwen R, Vrijbloed JW, van Der Meijden P, Dijkhuizen L. 2000. Targeted disruption of the kstD gene encoding a 3-ketosteroid delta(1)-dehydrogenase isoenzyme of rhodococcus erythropolis strain sq1. *Appl Environ Microbiol* 66:2029–2036. <https://doi.org/10.1128/AEM.66.5.2029-2036.2000>
  65. Griffin JE, Pandey AK, Gilmore SA, Mizrahi V, Mckinney JD, Bertozzi CR, Sasseti CM. 2012. Cholesterol catabolism by *Mycobacterium tuberculosis* requires transcriptional and metabolic adaptations. *Chem Biol* 19:218–227. <https://doi.org/10.1016/j.chembiol.2011.12.016>
  66. Yu CP, Roh H, Chu KH. 2007. 17  $\beta$ -estradiol-degrading bacteria isolated from activated sludge. *Environ Sci Technol* 41:486–492. <https://doi.org/10.1021/es060923f>
  67. Horinouchi M, Hayashi T, Kudo T. 2012. Steroid degradation in comonomas testosteronei. *J Steroid Biochem Mol Biol* 129:4–14. <https://doi.org/10.1016/j.jsbmb.2010.10.008>
  68. Belic I, Socic H. 1972. Microbial dehydrogenation of tomatidine. *J Steroid Biochem* 3:843–846. [https://doi.org/10.1016/0022-4731\(72\)90037-4](https://doi.org/10.1016/0022-4731(72)90037-4)
  69. Belic I, Hirsil-Pintaric V, Socić H, Vranjek B. 1975. Microbial cleavage of the tomatidine spiroketal sidechain. *J Steroid Biochem* 6:1211–1212. [https://doi.org/10.1016/0022-4731\(75\)90107-7](https://doi.org/10.1016/0022-4731(75)90107-7)
  70. Bowyer P, Clarke BR, Lunness P, Daniels MJ, Osbourn AE. 1995. Host-range of a plant-pathogenic fungus determined by a saponin detoxifying enzyme. *Science* 267:371–374. <https://doi.org/10.1126/science.7824933>
  71. Melton RE, Flegg LM, Brown JKM, Oliver RP, Daniels MJ, Osbourn AE. 1998. Heterologous expression of *Septoria lycopersici* tomatinase in *Cladosporium fulvum*: effects on compatible and incompatible interactions with tomato seedlings. *Mol Plant Microbe Interact* 11:228–236. <https://doi.org/10.1094/MPMI.1998.11.3.228>
  72. Shimasaki T, Masuda S, Garrido-Oter R, Kawasaki T, Aoki Y, Shibata A, Suda W, Shirasu K, Yazaki K, Nakano RT, Sugiyama A, Guttman DS. 2021. Tobacco root endophytic arthrobacter harbors genomic features enabling the catabolism of host-specific plant specialized metabolites. *mBio* 12:e0084621. <https://doi.org/10.1128/mBio.00846-21>
  73. Huang AC, Jiang T, Liu Y-X, Bai Y-C, Reed J, Qu B, Goossens A, Nützmann H-W, Bai Y, Osbourn A. 2019. A specialized metabolic network selectively modulates Arabidopsis root microbiota. *Science* 364:eaa06389. <https://doi.org/10.1126/science.aau6389>
  74. Wei GF, Chen ZJ, Wang B, Wei FG, Zhang GZ, Wang Y, Zhu GW, Zhou YX, Zhao QH, He MJ, Dong LL, Chen SL. 2021. Endophytes isolated from *Panax notoginseng* converted ginsenosides. *Microb Biotechnol* 14:1730–1746. <https://doi.org/10.1111/1751-7915.13842>
  75. Okutani F, Hamamoto S, Aoki Y, Nakayasu M, Nihei N, Nishimura T, Yazaki K, Sugiyama A. 2020. Rhizosphere modelling reveals spatiotemporal distribution of daidzein shaping soybean rhizosphere bacterial community. *Plant Cell Environ* 43:1036–1046. <https://doi.org/10.1111/pce.13708>
  76. Bulgarelli D, Rott M, Schlaeppi K, Ver Loren van Themaat E, Ahmadinejad N, Assenza F, Rauf P, Huettel B, Reinhardt R, Schmelzer E, Peplies J, Gloeckner FO, Amann R, Eickhorst T, Schulze-Lefert P. 2012. Revealing structure and assembly cues for Arabidopsis root-inhabiting bacterial microbiota. *Nature* 488:91–95. <https://doi.org/10.1038/nature11336>

77. Bai Y, Müller DB, Srinivas G, Garrido-Oter R, Potthoff E, Rott M, Dombrowski N, Münch PC, Spaepen S, Remus-Emsermann M, Hüttel B, McHardy AC, Vorholt JA, Schulze-Lefert P. 2015. Functional overlap of the Arabidopsis leaf and root microbiota. *Nature* 528:364–369. <https://doi.org/10.1038/nature16192>
78. Devers M, Soulas G, Martin-Laurent F. 2004. Real-time reverse transcription PCR analysis of expression of atrazine catabolism genes in two bacterial strains isolated from soil. *J Microbiol Methods* 56:3–15. <https://doi.org/10.1016/j.mimet.2003.08.015>
79. Hahn M, Henneke H. 1984. Localized mutagenesis in *Rhizobium japonicum*. *Molec Gen Genet* 193:46–52. <https://doi.org/10.1007/BF00327412>
80. Hunt M, Silva ND, Otto TD, Parkhill J, Keane JA, Harris SR. 2015. Circlator: automated circularization of genome assemblies using long sequencing reads. *Genome Biol* 16:294. <https://doi.org/10.1186/s13059-015-0849-0>
81. Aramaki T, Blanc-Mathieu R, Endo H, Ohkubo K, Kanehisa M, Goto S, Ogata H. 2020. Kofamkoala: KEGG ortholog assignment based on profile HMM and adaptive score threshold. *Bioinformatics* 36:2251–2252. <https://doi.org/10.1093/bioinformatics/btz859>
82. Shilling PJ, Mirzadeh K, Cumming AJ, Widesheim M, Köck Z, Daley DO. 2020. Improved designs for pET expression plasmids increase protein production yield in *Escherichia coli*. *Commun Biol* 3:214. <https://doi.org/10.1038/s42003-020-0939-8>
83. Page AJ, Cummins CA, Hunt M, Wong VK, Reuter S, Holden MTG, Fookes M, Falush D, Keane JA, Parkhill J. 2015. Roary: rapid large-scale prokaryote pan genome analysis. *Bioinformatics* 31:3691–3693. <https://doi.org/10.1093/bioinformatics/btv421>
84. Katoh K, Standley DM. 2013. MAFFT multiple sequence alignment software version 7: improvements in performance and usability. *Mol Biol Evol* 30:772–780. <https://doi.org/10.1093/molbev/mst010>
85. Price MN, Dehal PS, Arkin AP. 2009. Fasttree: computing large minimum evolution trees with profiles instead of a distance matrix. *Mol Biol Evol* 26:1641–1650. <https://doi.org/10.1093/molbev/msp077>
86. Letunic I, Bork P. 2007. Interactive tree of life (iTOL): an online tool for phylogenetic tree display and annotation. *Bioinformatics* 23:127–128. <https://doi.org/10.1093/bioinformatics/btl529>
87. Bray NL, Pimentel H, Melsted P, Pachter L. 2016. Near-optimal probabilistic RNA-seq quantification. *Nat Biotechnol* 34:525–527. <https://doi.org/10.1038/nbt0816-888d>